ABSTRACT

Title of Document: AN INVESTIGATION OF THE UL-94V
PLASTICS FLAMMABILITY TEST

Brian P. Downey, Master of Science
in Fire Protection Engineering, 2009

Directed by: J.L. Bryan Professor Dr. James G. Quintiere
Department of Fire Protection Engineering

The UL-94 Vertical Burning Flammability Test (UL-94V) is used to measure flammability characteristics of plastic materials. The results of the test allow for plastic materials to be separated into classification categories. These categories will be discussed and related to fire phenomena. Simulations of the test have allowed for the development of general flame height and heat flux correlations. We believe these are independent of the actual solid fuels. In addition, the heat flux from the ignition burner, a specified premixed flame, has been measured. These data provide the basis for assessing fire behavior of materials using their fire properties such as heat of combustion, heat of gasification, ignition temperature, and thermal properties. Criteria for ignition, sustained burning, and flame spread are determined. These outcomes are then related to the UL-94V classification categories. An analysis of melting is also considered in order to assess the flaming drip aspect of the test.

AN INVESTIGATION OF THE UL-94V PLASTICS
FLAMMABILITY TEST

by

Brian P. Downey

Thesis submitted to the Faculty of the Graduate School of the
University of Maryland, College Park in partial fulfillment
of the requirements for the degree of
Master of Science
2009

Advisory Committee:
Professor James Quintiere, Chair/Advisor
Professor James Milke
Assistant Professor Peter Sunderland

Acknowledgments

Table of Contents

List of Tables

List of Figures

Chapter 1

Introduction

1.1 Background and Motivation

The UL-94 Flammability Test [1] published by Underwriter's Laboratories is one of the available pre-selection test programs conducted on plastic materials to measure flammability characteristics. This test determines the tendency of a material either to extinguish or to spread a flame, presuming that the specimen has been ignited by an applied premixed flame.

The Federal Aviation Administration is interested in gaining a greater understanding of the UL-94 Test, including the fire phenomena and material properties governing the results. Although the UL-94 test is one of the few widely used flammability standards for plastic materials in consumer products, the extent to which the UL-94 test measures the fire hazard of a material is disputed. A more complete understanding of the applicability of the test would be beneficial to efforts aimed at reducing the fire hazard of consumer products.

The UL-94 Flammability Test [1] is actually comprised of six separate tests that can be performed independently. These tests yield separate classifications of the flammability of plastic materials used for parts in devices and appliances. This study will focus on the UL-94V: Vertical Burning Test.

1.2 Vertical Burning Test; 94V-0, 94V-1, 94V-2

The following sections will describe the test specimens, test setup, procedure and test criteria of the Vertical Burning Test (UL-94V). The Vertical Burning Test is conducted on small bar specimens mounted with their longitudinal axis oriented vertically. A 20 mm tall premixed methane flame is applied to the bottom edge of the specimen. The test yields ratings for materials tested of V-0, V-1, and V-2 (listed from most to least desirable) [1].

It should be noted that five (5) specimens of each material are tested. If a trial for any one sample of the material performs worse, i.e., results in a lower rating, than the other four, a second set of 5 can be tested. If any of these specimens still yields an inconsistent result, then the material shall be classified by this lower rating [1].

A material that does not meet the criteria of the Vertical Test can be tested and classified in accordance with UL-94HB: Horizontal Burn Test [1]. The Horizontal Burn Test measures the burning rate of horizontally mounted specimens [1].

1.2.1 Specimens

The standard bar specimens are required to be cut from sheet materials, or to be molded to the necessary form [1]. If one cuts the bar sample from a larger plastic sheet, all dust and particles must be removed from the surface of the material and the edges of the finished specimen must be given a smooth finish. The author suggests that the presence of plastic "burs" would likely impact results of the test

Figure 1.1: PEI and PVC UL-94V Samples

by making it easier for the sample to ignite.

The standard bar specimen is to be 125 ± 5 mm long and 13.0 ± 0.5 mm wide [1]. The sample is to also be provided in minimum and maximum thicknesses of the material as manufactured; the maximum accepted thickness is 13 mm [1]. Further, if the results for minimum and maximum thicknesses demonstrate a need, presumably by yielding different results, intermediate thicknesses can be tested to resolve the disagreement [1]. The corner of the sample should be rounded but the corner radius cannot exceed 1.3 mm [1]. Samples of of PEI and PVC are shown in Fig. 1.1. An engineering drawing of the standard specimen is provided in Appendix A.

Testing conducted by the author under the guidance of an FAA technician at the William J. Hughes Technical Center (WJHTC) in Atlantic City, New Jersey resulted in two additional specimen preparation notes. First, one should be sure to remove the plastic wrapping present on some of the materials. It is also advisable to wipe the prepared sample with a cloth after mounting it; removing any oils transferred from the skin of the technician that could adversely affect the results of the test.

The samples are required to be preconditioned in accordance with ASTM D618 (ISO 291) at 23 ± 2 °C and 50 ± 5 % relative humidity for a minimum of 48 hours [1]. When conducting the UL-94V test at the WJHTC, conditioning was approximated by storing the samples in an environmentally controlled storage room where the humidity was regulated.

1.2.2 Test Setup

Fig. 1.2 shows the test setup as provided within the UL-94 Standard for the Vertical Burning Test [1]. The various components of the test setup are then described in the following sections, including how the mount the specimen, characteristics of the fume hood under which the test is conducted, the burner used, and the gas supply required.
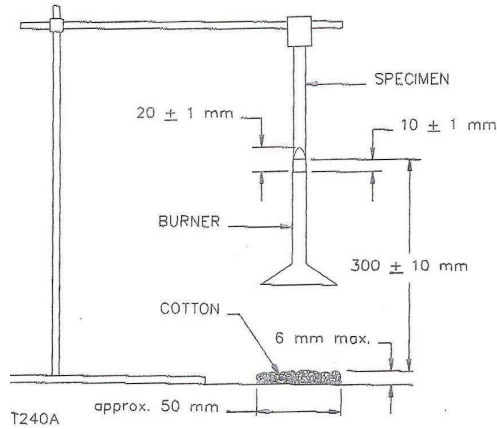
Figure 1.2: UL-94V Test Setup Diagram[1]

1.2.2.1 Mounting the Specimens

As mentioned previously, the specimen is to be mounted with the longitudinal axis oriented vertically. The bottom edge of the specimen must be 300 ± 10 mm above a horizontal layer of approximately 0.08 grams of cotton [1]. The piece of cotton placed on the surface below the specimen should be approximately 50 mm long and 50 mm wide, with a maximum thickness of 6 mm [1]. If flaming drips of material produced during the test fall and ignite the cotton, the rating of the sample is at best classified as a V-2 material. Further discussion of the rating system is included in the Procedure Section.

1.2.2.2 Fume Hood

The laboratory fume hood is required to have a minimum volume of 0.5 m^3 [1]. The hood being used must allow for one to observe the test while also preventing air

drafts that could adversely affect the results. An air evacuation device is necessary to remove the products of combustion, which may be toxic. This evacuation device must be turned off during the actual test [1].

1.2.2.3 Burner

A laboratory type burner having a tube with length 100 ± 10 mm and an inside diameter of 9.5 ± 0.3 mm is required by the standard. Further, the burner is to be in compliance with ASTM D5025 [2]. ASTM D5207 [3] provides a procedure to verify the appropriate flame conditions through temperature measurement using a copper slug.

1.2.2.4 Gas Supply

A supply of technical grade methane gas (minimum 98 percent pure) with regulator and meter for uniform gas flow is required [1]. A flow rate of 105 mL/min is specified to produce the 20 mm methane premixed flame for the burner used [1].

1.2.3 Procedure

After both mounting the sample as described previously and validating the characteristics of the methane premixed flame, one should position the burner so that the flame is applied centrally to the middle point of the bottom edge of the specimen. The top of burner tube should be 10 ± 1 mm below the bottom edge of the specimen [1]. Because the height of the flame is 20 mm, bisecting the height of

the flame is a good visual cue for appropriately positioning the burner.

The technician should hold the burner in place, maintaining a 10 mm distance from the top of the burner tube to the bottom of the specimen for 10 ± 0.5 s; hereby referred to as the first flame application. In the event that the specimen burns away or curls away from the burner, one follows the specimen in order to maintain the 10 mm distance [1]. If the specimen drips molten or flaming material while the flame is being applied, the burner can be tilted up to an angle of 45° in order to prevent the material dropping from the sample and entering the tube of the burner[1].

After the first flame application, the burner is to be withdrawn at a rate of approximately 300 mm/s to a distance of at least 150 mm away from the specimen [1]. At the moment when the flame is removed, one commences measuring the after-flame time, referred to as t_1 in the standard. The afterflame time is the total time during which flaming material persists after the ignition source has been removed[1].

If it is difficult to determine the presence of flaming material rather than glowing material, a small piece of cotton, held by a pair of tweezers for safety, should be brought into contact with the area of the specimen in question. Ignition of this cotton indicates the presence of flaming material [1].

As soon as flaming combustion of the specimen ceases, even if the burner has not been withdrawn to the full 150 mm distance from the specimen, the top of the burner tube is immediately placed under the specimen at a distance of 10 ± 1 mm away from the bottom edge of the specimen [1]. This second flame application continues for 10 ± 0.5 s. The same recommendations given for the first flame application regarding tilting the burner and maintaining the prescribed distance

remain.

After the conclusion of the second flame application, the burner is again removed at a rate of approximately 300 mm/sec to a distance of at least 150 mm away from the specimen. At the moment when the flame is removed, the technician should commence measuring the afterflame time, t_2, and the afterglow time, t_3 [1]. The afterglow time is the length of time for which a material continues to glow under specified test conditions, after the ignition source has been removed and/or cessation of flaming [1].

In addition to the times t_1, t_2, and t_3, the technician should record whether the specimen burns up to the holding clamp and whether the specimen drips flaming particles that ignite the cotton indicator [1].

A special note is given in the standard regarding the extinguishment of the premixed flame during the flame application. If the test flame is extinguished during either of the two flame applications, the test specimen is to be disregarded and another specimen is to be tested[1]. The only exception is in the case where the test flame is extinguished as a direct result of out-gassing from the specimen. In this case, the burner shall be reignited immediately and reapplied to the specimen so that the total time of application is 10 ± 0.5 seconds [1].

1.2.4   Classification Criteria

Classification of a tested material as a V-0, V-1, or V-2 material is in part based on the times t_1, t_2, and t_3 recorded during the test. Other criteria include the

presence of flaming drips which cause the cotton indicator to ignite and whether the material burns all the way to the holding clamp[1].

Table 1.1 shows the timing requirements, as well as the necessary observed dripping and melting behaviors, that must be met in order to be classified as a V-0, V-1, or V-2 material[1]. V-0 materials include those samples that do not ignite or that extinguish the flame within a 10 s after removal of the premixed flame. V-1 materials include samples that extinguish the flame within 30 seconds and do not allow for flame propagation up the holding clamp. V-2 materials have the same timing requirements as V-1 but are allowed to produce flaming drips which ignite the cotton placed below the specimen. A material that does not pass UL-94V and is often subsequently tested according to UL-94HB, sustain burning for greater than 30 seconds or allow flame propagation to the holding clamp.

The author has designed the following flow chart (Fig. 1.3) in an attempt to connect the rating system and fire phenomena underlying the results of the test by graphically displaying the criteria and subsequent ratings of the tested materials. The boxes labeled as "No Rating" show that the material does not pass the UL-94V test.

It is possible to directly relate the criteria of the UL-94V test with the fire phenomena of ignition, sustained burning, and flame spread. By defining a characteristic time, t_{flame}, as the time over which flaming material persists after the ignition source has been removed, one can relate the criteria of the test directly to these fire phenomena. Table 1.2 lists this time, t_{flame}, the resulting UL-94V rating, and the related fire phenomenon.

9

Table 1.1: Materials Classifications [1]

Criteria Conditions	V-0	V-1	V-2
Afterflame time for each individual specimen, t_1 or t_2	≤ 10 s	≤ 30 s	≤ 30 s
Total afterflame time for any condition, $(t_1 + t_2)$ for the 5 specimens	≤ 50 s	≤ 250 s	≤ 250 s
Afteflame plus afterglow time for each individual specimen after the second flame application $(t_2 + t_3)$	≤ 30 s	≤ 60 s	≤ 60 s
Afterflame or afterglow of any specimen up to the holding clamp	No	No	No
Cotton indicator ignited by flaming particles or drops	No	No	Yes
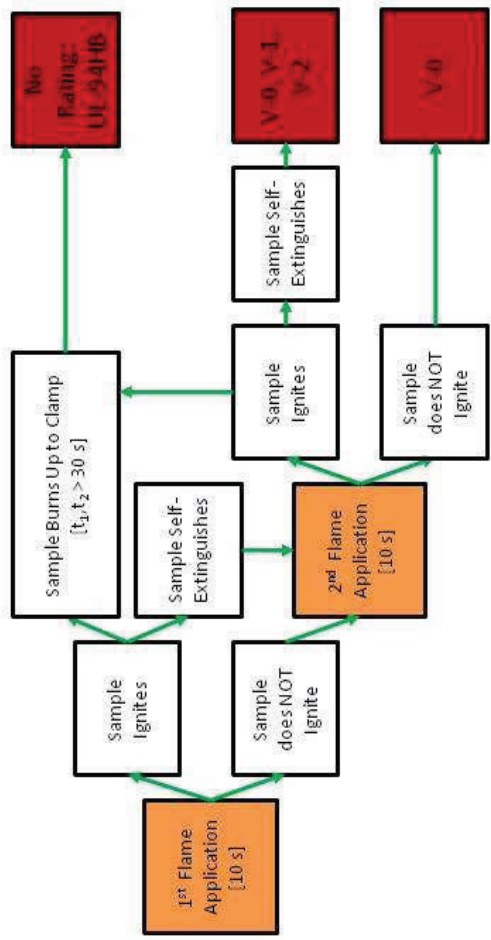
Figure 1.3: UL-94V Flow Chart

Table 1.2: Relating UL-94V Ratings to Fire Phenomena

t_{flame}	UL-94V Rating	Fire Phenomena
≤ 10 s	V-0	Material does not or barely ignites
10 s $\leq t_{flame} \leq 30$ s	V-1 or V-2	Burning is not sustained
> 30 s	HB	Burning is sustained
		Material burns up to holding clamp

1.3   Literature Review

Interest in understanding the UL-94 Test is not unprecedented. Section 1.3.1 highlights some relevant previous studies; including the work of Dr. Richard Lyon of the Federal Aviation Administration.

By comparing the rating criteria of the UL-94V test to distinct fire phenomena, including ignition, sustained burning and flame spread, it is possible that empirical correlations could be used to predict the behavior of materials being tested. The analysis contained herein will follow successful methods that were used to understand fire phenomena of burning walls. These previous correlations between heat release rate, flame height, and heat flux for vertical burning walls may be helpful in understanding the vertical burning seen during the UL-94V test. Section 1.3.2 describes some of these empirical correlations for burning walls.

1.3.1   Previous Related Studies

While presenting a broad narrative on the ignition research that has been conducted over the last century, Babrauskas [4] mentioned the importance of understanding small-scale flame tests, specifically UL-94. Although he said that significant progress in quantifying heat flux from flames has been made, the response of ma-

terial to non-uniform heating from a flame has not been explored at all. Further, Babrauskas [4] claims that no paper has attempted to model the ignition process that takes place when one of the flames specified in the UL-94 test is applied to the specimens. Although Babrauskas recognized the difficulty in modeling the ignition of these small specimens that are not uniformly heated, he pointed out that the flame used in the UL-94V test is representative of some flames that ignitable materials may encounter in real life.

Many of the previous investigations into UL-94V have attempted to correlate the results of the UL-94V test with other accepted test methods. Several investigations, including those by Morgan et al. [5], Hong et al. [6], and Schartel et al. [7], attempted to correlate results from the cone calorimeter test with results from the UL-94V test. These studies did not yield an indisputable relationship between the two tests. In fact, Morgan et al. [5] concluded that while both tests measure flammability, they do so differently, and therefore quantitative correlation between the two tests is not perfect [5].

Bundy and Ohlmeiller [8] have investigated the relationship between bench-scale and full-scale fire performance. The bench scale flammability tests included the cone calorimeter test (ASTM E 1354), the UL-94 Vertical Burn Test, and the Glow Wire Ignitability Temperature test (GWIT) (IEC 695-2-1/3). The authors concluded that it is likely that both UL-94 performance and the rate of heat release measurements are necessary to predict how materials can be expected to react in a real fire hazard scenario.

Lyon [9] has argued that the probability that a plastic sample will fail the UL-

94V test can be determined from a 3 mg sample burned in the microscale combustion calorimeter.

Lyon has also presented a method that can be used to gain an understanding of the relationship between the fire behavior of plastics and their properties [10]. By identifying flammability values that can be measured and tabulated, Lyon predicts the fire hazard for plastic materials. One such property, the Heat Release Parameter (HRP), can be used to predict an ideal or intrinsic heat release rate, HRR_o. The Heat Release Parameter is the ratio of the heat of combustion to the heat of gasification, $\Delta h_c/L$. As a result, the heat release rate of plastic can be expressed in terms of an intrinsic heat release rate in unforced flaming combustion and an extrinsic heat release rate: $HRP \times \dot{q}_{ext}$. It should be noted that $\dot{q}_{ext}$ is the net total incident heat flux to the surface of the material.

The heat release rate for flaming combustion, $\dot{Q}$, follows in Eq. 1.1:

$$\dot{Q} = \chi \Delta h_c \dot{m}_g''$$
(1.1)

where χ is the gas phase combustion efficiency, Δh_c is the net heat of complete combustion of the material's pyrolysis gases, and $\dot{m}_g''$ is the pyrolysis rate per unit surface area.

In his calculation of the heat release rate for flaming combustion, Lyon [10] also accounts for the portion of the material that does not pyrolyze:

$$\dot{Q} = \chi(1 - \mu)\Delta h_c \dot{m}_g''$$
(1.2)

where μ is the inert fraction of char residue.

14

If one assumes steady burning, then:

$$\dot{m}_g = \frac{\dot{q}_{net}}{h_g} \qquad (1.3)$$

$$\dot{Q} = \chi(1-\mu)\frac{\Delta h_c}{h_g}\dot{q}_{net} \qquad (1.4)$$

Therefore, one can express the heat release rate for flaming combustion in terms of the HRP.

$$\dot{Q} = HRP \times \dot{q}_{net} \qquad (1.5)$$

where $HRP = \chi(1-\mu)\Delta h_c h_g$.

The expression for $\dot{q}_{net}$ is the sum of the incident external radiant heat flux from an external source, the incident heat flux from the flame of the material, and the total losses. The total losses include the loss through conduction to the portion of the sample not being heated and the loss through re-radiation. It is at this point that Lyon [10] defines the intrinsic heat release rate, where the incident heat flux from an external source is equal to zero.

$$\dot{Q} = HRP \times (\dot{q}_{ext} + \dot{q}_{flame} - \dot{q}_{loss}) \qquad (1.6)$$

If the $\dot{q}_{ext} = 0$, then

$$HRR_o = HRP \times (\dot{q}_{flame} - \dot{q}_{loss}) \qquad (1.7)$$

In summary,

$$\dot{Q} = HRR_o + HRP \times (\dot{q}_{ext}) \qquad (1.8)$$

The term HRR_o has the units and significance of an ideal or intrinsic heat release rate of the material burning under ambient (unforced) conditions [10] that

15

Table 1.3: Comparison of HRR_o to Accepted Ratings [10]

Material	HRR_o (kW/m^2)	Accepted Rating
PPS	-147±30	V-0
ECTFE	-127±6	V-0
PEEK	-94±20	V-0
PTFE	-84±9	V-0
PAI	-64±16	V-0
CPVC	-34±9	V-0
PVCR	9±25	V-0
ETFE	44±31	V-0
PC	89±32	V-2
POM	162±30	HB
PA6	187±55	HB
PMMA	217±47	HB
PA66	240±59	HB
UPT	261±105	HB
PBT	341±106	HB
ABS	359±66	HB
PP	369±79	HB
PS	410±66	HB
PET	424±168	HB
HIPS	510±77	HB

can be extrapolated from cone calorimeter tests. Lyon then compares the HRR_o of common polymeric materials with the UL-94 rating of that material in order to determine a critical heat release rate for sustained burning. Table 1.3 shows the HRR_o calculated by Lyon [10] along with the accepted UL-94 rating of some common materials [10]. For HRR_o of greater than 90 kW/m^2, materials sustain burning and do not attain a V-rating. For HRR_o below approximately 44 kW/m^2, materials appear to achieve a V-0 rating.

1.3.2 Empirical Correlations for Burning Walls

The following correlations for heat transfer and flame spread can be used to predict ignition and flame spread for burning walls. This study aims to produce similar correlations that relate specifically to the UL-94V test.

Researchers have developed correlations between the flame heat flux transferred ahead of the pyrolysis front and heat release rate for downward, upward, and horizontal fire propagation [11, 12]. Most importantly, Fernandez-Pello and Hirano [12] used analysis from Alpert [13] to corroborate that heat transfer from the flame to the fuel is the controlling mechanism in the wind-aided mode of flame spread.

A literature review by Lattimer [14] showed that some researchers have used line burners to simulate a fire produced by a vertical burning surface. For example, Hasemi [15] measured the heat flux from a methane line burner to an incombustible wall. In his experiments, Hasemi varied the fire heat release rate per unit length of the line burner from 16.7-218.2 kW/m for two different line burner widths: 0.037 m and 0.082 m.

In tests using propane with $\dot{Q}' = 83$ - 167 kW/m, Kokkala et al. [16] and Lattimer [17] both measured heat fluxes of approximately 45 kW/m^2 in the lower half of the flame ($z = 0.5L_f$). Foley and Drysdale [18] measured 40-50 kW/m^2 from propane line burners with $\dot{Q}' = 11.6$ and 20.9 kW/m. These data indicate that the radiation from the flame to the surface is dependent on fuel soot production. Therefore, the radiation fraction of the flame for the material being tested may have an impact on the heat flux to the surface.

17

Work by Ahmed and Faeth [19], who correlated their heat flux data using a turbulent flame-sheet model based on convective heating alone, found by measurements that the convective component of heating was nearly 80 to 90% of the total heat flux. In contrast, work by Orloff [20] for flame spread on polymethylmethacrylate shows a radiative component of 50 to 75%. Thus the composition of the heat flux is expected to be material and scale dependent [14].

Correlations published previously by Hasemi [21, 22, 23], Mitler [24], and Williams et al. [25] have assumed a constant heat flux in the lower part of the flame and power law decay above a certain flame height, typically taken as one-half of the greatest height measured. The correlations given in the literature vary in the peak heat flux recorded and in the power-law empirical constant, which governs the decay. These empirical values depend on several factors, including the fuel used and dimensions of the burning specimen.

Tewarson [26] describes how the relationship between flame height and the position of the pyrolysis front of a burning wall can be used to predict flame spread. The equation relating the flame height, x_f, and the position of the pyrolysis front, x_p, is as follows:

$$x_f = a(x_p)^n \qquad (1.9)$$

Fire propagation data for PMMA from the ASTM E2058 [27] fire propagation apparatus and for electrical cables from several standard test for cables [11] yield empirical values for a and n in Eq. 1.9 of 5.35 and 0.67-0.80, respectively. Here, both x_f and x_p are given in meters.

Additional research has shown that an equation of the same form as Eq. 1.9 can relate the normalized chemical heat release to the ratio of the flame height to the pyrolysis position, as shown in Eq. 1.10 [26]. The ratio of the flame height to pyrolysis front is a good indicator of the fire propagation characteristics of the materials [26]. Further, materials for which flame height is close to the pyrolysis front during fire propagation can indicate decelerating fire propagation behavior.

$$\frac{x_f}{x_p} = a[NCHRR]^n \tag{1.10}$$

where $NCHRR$, normalized chemical heat release rate, is defined as:

$$NCHRR = \frac{\dot{Q}'}{\rho c_p T_a \sqrt{g} x_p^{3/2}} \tag{1.11}$$

Data for diffusion flames can be characterized for distinct values of n in Eq. 1.10. For methane combustion and a normalized chemical heat release rate of between 0.2 and 5, the ratio of the flame height to the pyrolysis position lies between 1.5 and 20, following a 2/3 power law behavior [26].

Another method for predicting flame spread on a vertical surface was proposed by Quintiere, et al. [28] in which the burning wall was replaced with an incombustible material and then a flame, produced by a line burner, was applied. Quintiere, et al. then measured the height of the visible flame tips and the energy release rate per wall fire width:

$$\dot{E}' = \dot{E}'' x_p \tag{1.12}$$

This expression is important because Delichatsios has shown that flame height is solely dependent on energy release rate for wall fires [29].

19

1.4   Objectives

This study examines the burning behavior of materials tested in accordance with the UL-94V Flammability Test in order to gain a better understanding of the fire phenomena and material properties governing the results of the test. Also, an analysis of the variance in the test due to human error will be conducted.

To gain the desired understanding of this test, correlations relating the heat release rate, flame height, and heat flux to the plastic specimens are needed. These correlations will aid in predicting the behavior of the material being tested; including whether the sample ignites, sustains burning, or the flame spreads beyond the initial burning region. It is proposed that the heat release rate for a burning polymeric material can be compared to critical heat release rates for sustained burning and flame spread to predict material performance.

Chapter 2

Experimental Facilities

The following experimental facilities, including two flow meters, a Tirrill Burner, and a heat flux gauge, were used in conducting both the UL-94V test and the experiments described in Chapter 5 and Chapter 7.

2.1   Omega Flow Meters

Two high-accuracy shield rotameters, the FL-110 and the FL-112, from Omega Engineering, Inc., were used to measure the flow rate of methane gas. The FL-110 and FL-112 rotameters, shown in Fig. 2.1, have different cross-sectional areas thereby increasing the range of flow rates that could be measured.

These rotameters each included both a stainless steel and a glass float. The difference in the mass between the floats due to the difference in density between glass and stainless steel further increased the range of flow rates that could be measured. Fig. 2.2 shows the stainless less float and the glass float from the FL-112. Further, the floats used in the FL-110 were much smaller, and thus had a lower mass, than those from the FL-112, as shown in Fig. 2.3.

Omega Engineering, Inc. also provided flow tables to correlate the position of the float with a flow rate in mL/min. These tables were generated specifically for methane fuel, using a density of 0.6569 mg/mL and a viscosity of 10.919×10^{-3} cp. The volumetric flow rates were calculated for standard temperature and pressure. The correlated flow

Figure 2.1: FL-110 and FL-112 Rotameters

Figure 2.2: Stainless Steel and Glass Floats for FL-112 Rotameter

Figure 2.3: Stainless Steel Floats for FL-110 and FL-112 Rotameters
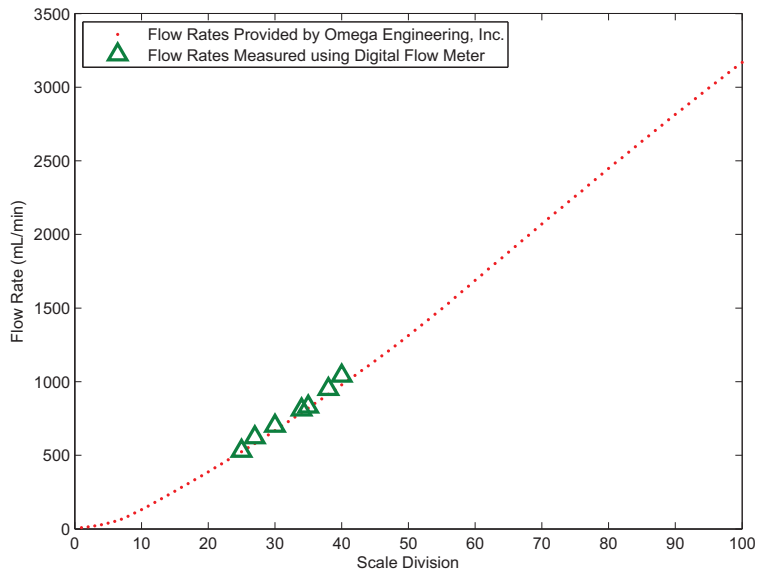
Figure 2.4: FL-112 Flow Rate Measurement Verification

tables for methane for both rotameters are available in Appendix B.

Verification of the accuracy of the flow tables provided by Omega Engineering, Inc. was achieved by connecting the FL-112 rotameter in-line with another flow meter whose accuracy had been previously verified. A plot of the data points taken from this test for the FL-112 and the points provided by Omega Engineering, Inc. can be seen in Fig 2.4.

2.2 Tirrill Burner

In an effort to standardize the results of the test, the Tirrill Burner being used satisfies specific design requirements. These requirements are detailed in the ASTM D 5025 [2]. The diameter of the burner barrel, the length of the burner barrel, the size of the burner orifice, and the dimensions of the needle valve are among the design features

standardized. Humboldt Manufacturing sells the H-5025 Tirrill Burner which satisfies the requirements of the standard (Fig. 2.6).

Humboldt Manufacturing also provided two burner tubes, one to lock out the air intake to produce a high yellow diffusion flame and the other to produce for a sharp blue premixed flame; the second of which is necessary for the UL-94V test. The burner tubes are shown in Fig. 2.7.
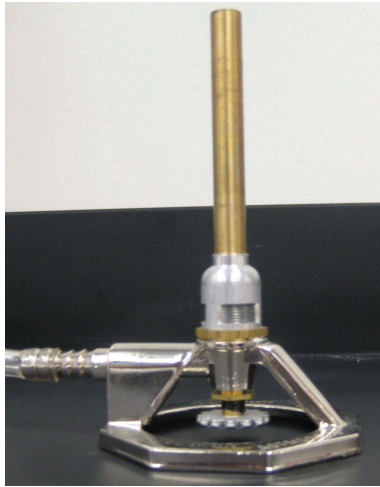
Figure 2.5: H-5025 Burner

Figure 2.6: Burner Tubes

2.3 Heat Flux Gauge

A $1/8^{th}$ inch diameter water-cooled heat flux gauge was used to measure the incident heat flux to the sample in the following experiments. An incident heat flux to the surface of the gauge causes a voltage difference to be created between the two lead wires. This voltage difference can then be converted to a measurement of kW/m^2 using a constant-slope relationship.

In order to verify the measurements being taken, the $1/8^{th}$ inch diameter water-

Figure 2.7: $1/8^{th}$ inch Diameter Heat Flux Gauge

cooled heat flux gauge was positioned near a propane burning wall. The voltage difference (in mV) as a result of the incident heat flux was measured at six different distances relative to the wall. Another heat flux gauge with a known voltage difference to heat flux relationship (2.08 mV/(kW/m^2)) was then used to measure the heat flux in the same six positions. This procedure allowed for the calculation of the voltage difference to incident heat flux relationship for the $1/8^{th}$ inch diameter heat flux gauge. The values used in calculating this constant-slope relationship are plotted in Fig. 2.9.
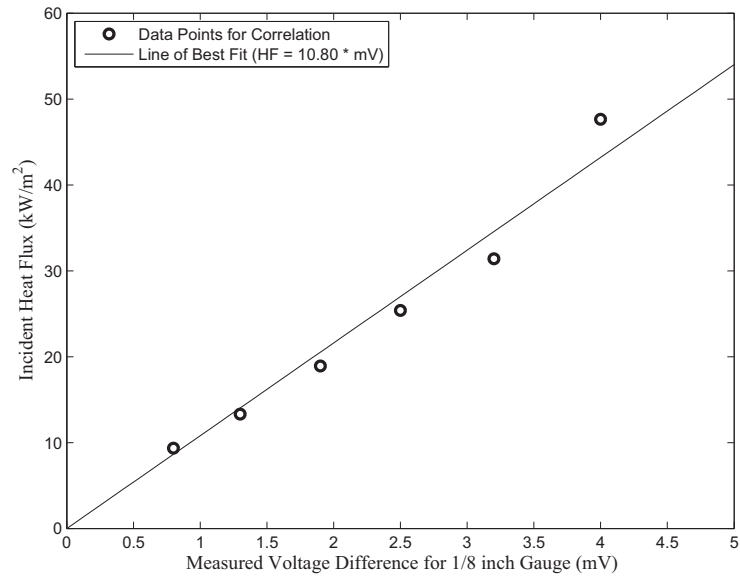
Figure 2.8: Heat Flux Gauge Correlation to Standard Measurement

Chapter 3

Ignition

The first fire phenomena that governs the results of the UL-94V test is ignition. If the material fails to ignite after the first or second flame application, then the material will pass the UL-94V test and be classified as a V-0 material. Therefore, the ability to predict the ignition behavior of plastic materials tested in accordance with UL-94V is extremely desirable. In this chapter, the 20 mm tall methane premixed flame will be characterized in terms of incident heat flux. The thermally-thin approximation will then be used in calculated ignition times for several common polymeric materials.

3.1   Experimental Methods to Characterize Applied Flame

It is speculated that variations in the incident heat flux, $\dot{q}''$, due to changes to distance from the burner to the specimen, orientation of the burner, and flow rate of methane fuel may compromise the results of the test by changing its ignition characteristics. Therefore, it becomes necessary to characterize the applied flame in terms of incident heat flux to more accurately model the ignition behavior of the plastic materials.

This section will summarize the experimental methods used to characterize the flame applied in the UL-94V test through measurements of the incident heat flux to the sample. A specimen with representative dimensions was fashioned from an incombustible material. A hole, with a diameter of 1/8 inch, was then cut into the specimen to allow for the heat flux gauge to be placed appropriately. The vertical position of the heat flux gauge was

varied between 0.5 cm and 1 cm, while the horizontal position remained along the vertical centerline of the mounted specimen. These vertical positions were chosen because the bottom region of the sample, where the flame is applied, will be the first to ignite during the test. The specimen was then clamped at the top edge and hung 300 mm above the surface of the laboratory table. The heat flux gauge was positioned such that its face was flush with the front face of the incombustible sample.

Using a NETDAQ data acquisition system, the voltage difference was measured at 0.01 second intervals for a 10 second trial. This data was recorded in a Microsoft Excel Spreadsheet, where the average and maximum values for the incident heat flux to the surface could be calculated for each experiment.

Figure 3.1 shows the burner placed directly below the specimen while Figure 3.2 shows the burner at a 45° angle to the specimen.
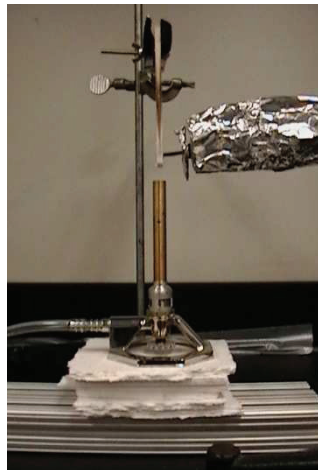
Figure 3.1: Burner Directly Below Sample   Figure 3.2: Burner 45° to Sample
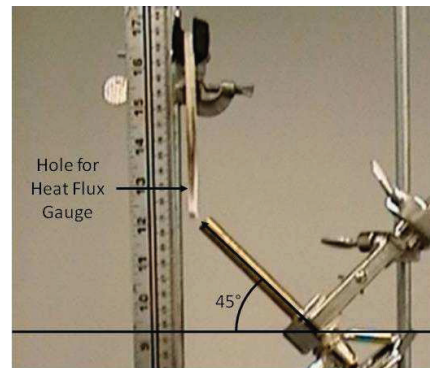
Figure 3.3 shows the time-average incident heat flux values for the burner both directly below and at 45° to the sample at heights of 0.5 and 1 cm. Also, the time-average incident heat flux to the bottom edge of the specimen was measured. The heat flux to the
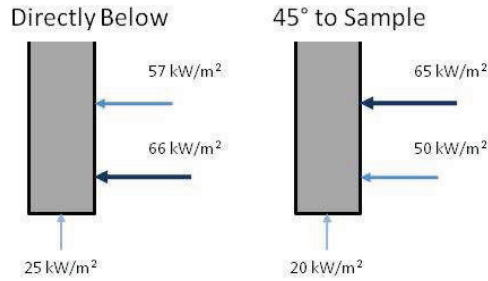
Figure 3.3: Time-Average Incident Heat Flux (Standard)

bottom edge of the specimen was only 20-25 kW/m^2 compared to 50-65 kW/m^2 along the faces of the specimen. Here, the flow rate of methane, flame height, and position of the burner were measured to comply with the requirements of the UL-94V test [1].

The following compares measurements of the incident heat flux taken for the setup given in the standard to measurements influenced by human factors, including changes in the flow rate of methane fuel, distance from the burner to the specimen, and the application angle. In the following plots, this controlled measurement of incident heat flux is referred to as the *Standardized Value*. To understand the human factors that could influence the incident heat flux to the materials, colleagues were asked to both adjust the premixed flame to the appropriate height and to apply the flame as prescribed in the standard for a 10 s period. Inherently, the application orientation and distance would vary from person to person. The incident heat flux value shown in the plot and labeled *Colleague Measurements* is a time-average value for all seven of the participants. The thickness of the incombustible specimen used in these measurements was 4.3 mm.

Because the UL-94V Standard [1] requires a methane flow rate of 105 mL/min that

29
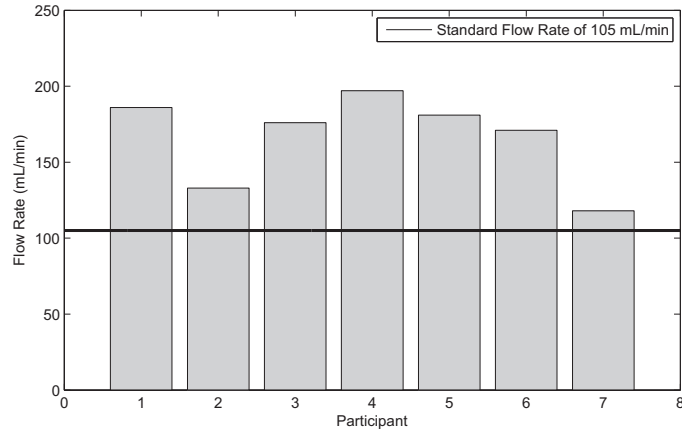
Figure 3.4: Actual flow rates based on flame height measurements

produces a 20 mm tall flame, some have used flame height as a method to verify the flow rate rather than actually measuring the flow rate itself. If one incorrectly measures the flame height of the premixed flame, then the flow rate will likely be incorrect. As such, each of the participants was asked to adjust the flow rate of the methane fuel until a 20 mm tall flame was achieved. The actual flow rate of methane was measured for each of the participants and plotted in Fig. 3.4. The actual flow rate for each participant can be compared to the methane flow rate prescribed by the UL-94V test standard of 105 mL/min [1]. Participants consistently overestimated the flow rate necessary to produce a 20 mm tall flame; the average flow rate for all seven of the participants was 166 mL/min. The maximum flow rate measured was 197 mL/min while the minimum flow rate measured was 118 mL/min.

Figure 3.5 shows the time-average incident heat flux measured for the burner positioned directly below the specimen for both the *Standardized Value* and the *Colleague Measurements*. The incident heat flux values at both 0.5 cm and 1 cm heights fall within

30
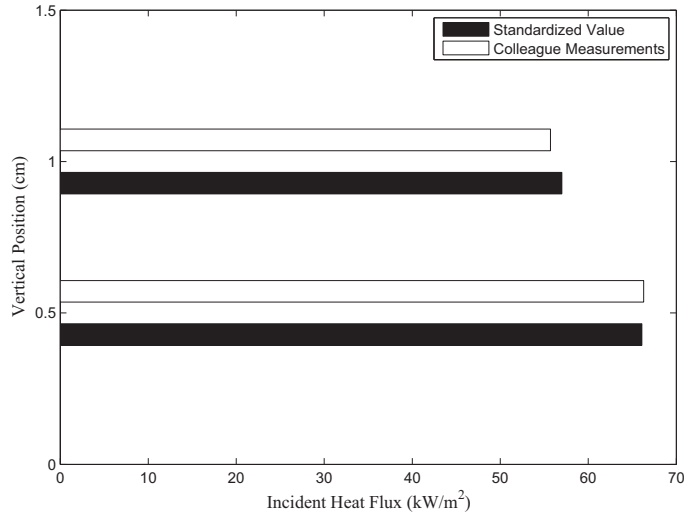
Figure 3.5: Average Incident Heat Flux with Burner Directly Below Specimen

2-3 kW/m^2 of one another. Considering the errors made in flow rate and the variability in the distance from the burner tube to the bottom edge of the sample, this variance is reasonable.

Figure 3.6 shows the time average incident heat flux measured for the burner positioned at 45° to the specimen for both the *Standardized Value* and the *Colleague Measurements*. At a height of 0.5 cm, the time-average value of the standardized incident heat flux is approximately 10 kW/m^2 (48.1 kW/m^2) less than the time-average value for all of the *Colleague Measurements* (58.9 kW/m^2). At a height of 1 cm, the time-average value of the standardized incident heat flux value is approximately 10 kW/m^2 (64.5 kW/m^2) greater than the time-average for all of the *Colleague Measurements* (56.3 kW/m^2). It is proposed that changes in application angle can significantly impact the incident heat flux, and thus the ignition of materials being tested in accordance with UL-94V.

Ultimately, one appropriate incident heat flux is needed to calculate the ignition
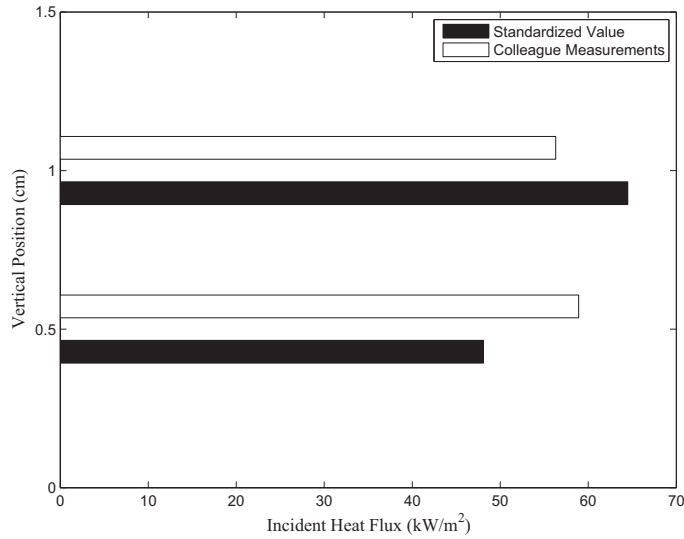
Figure 3.6: Average Incident Heat Flux with Burner at 45 Degrees to Specimen

time. From the measurements just described, an incident heat flux value of 60 kW/m^2 was used in calculating the ignition time of several common polymeric materials

3.2 Theoretical Basis for Predicting Ignition

If the thickness of the material is acceptably less than the thermal penetration depth, the material may be approximated as thermally-thin. The following analysis to determine the applicability of the thermally thin approximation was taken from a similar analysis done by Spearpoint and Quintiere [31]. When the premixed flame is applied directly below the specimen, the flame fully envelopes the bottom region of the sample, heating the material on both sides. It is then appropriate to determine the applicability of the thermally-thin approximation based on 1/2 of the specimen thickness. Fig. 3.7 shows the incident heat flux on both sides of a UL-94V specimen.
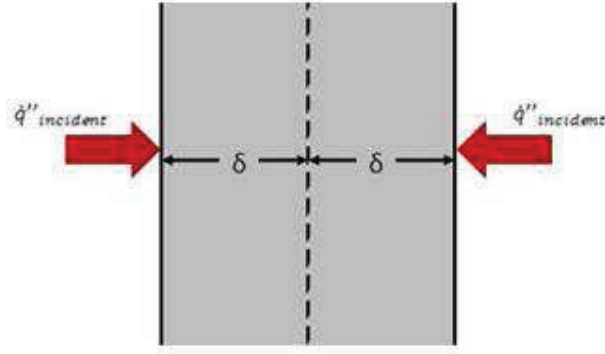
Figure 3.7: Heating of UL-94V Specimen - Thermally Thin Approximation

A critical thermal penetration depth, δ_{crit}, can be calculated as shown in Eq. 3.1:

$$\delta \leq \delta_{crit} = \frac{2k\Delta T}{\dot{q}''} \tag{3.1}$$

This critical value can then be compared to the thickness of the material to determine the applicability of the thermally-thin approximation.

Typically, the difference between either the melt, vaporization, or ignition temperature of a material with the ambient temperature is on the order of 200 to 300 K. For this calculation, the characteristic temperature difference, ΔT, is 250 K. The thermal conductivity, k, for polymers is typically on the order of 0.4 W/m-K. The characteristic value for net incident heat flux, $\dot{q}''$, is taken from the Section 3.1 as 60 kW/m^2. Then,

$$\delta_{crit} = \frac{2(0.4W/m - K)250K}{60000W/m^2} = 3.33mm \tag{3.2}$$

The thicknesses for several common polymeric materials that have been previously tested in accordance with UL-94V are given in Table 7.1 [30]. The thickness of these

Table 3.1: Common Polymers and Their Thicknesses [30]

Polymer	Thickness (mm)
Polyphenylene Sulfice (PPS)	6.5
Polyvinyl Chloride (PVC)	6.1
Polyamide 6,6 (PA66)	6.73
High-Impact Polystyrene (HIPS)	6.14
High-Density Polyethylene (HDPE)	6.35
Polyvinylidene Fluoride (PVDF)	6.63
Polyoxymethylene (POM)	6.75
Polycarbonate (PC)	5.35
Poly(methyl methacrylate) (PMMA)	5.35
Acrylonitrile butadiene styrene (ABS)	6.35
Polyetherimide (PEI)	6.85

materials shown in Table 3.1 is less than $2\delta_{crit}$, the materials included in this investigation are approximated as thermally-thin.

3.3 Applying Experimental Results to Theoretical Model

Because the temperature of the sample is increasing as the sample is being heated, a non-linear calculation of the ignition time for each material was used to increase the accuracy of the prediction. Eq. 3.3 can be used to predict the ignition time for materials using the net incident heat flux measured previously.

$$\rho c_p \delta \frac{dT}{dt} = \dot{q}''_{incident} - CHF)$$

(3.3)

The radiative losses occurring during the ignition process can be calculated for each of the materials as in Equation 3.4:

$$CHF = \epsilon\sigma(T_{ig}^4 - T_{\infty}^4)$$

(3.4)

The value for the incident heat flux used was 60 kW/m^2; taken from the measurements used to characterize the applied flame. The initial temperature of the surface is taken to be equal to that of the ambient environment. The temperature of the surface is then calculated at each time step based on the surface temperature at the previous time step. The total elapsed time is recorded until the surface temperature of the material is equal to the ignition temperature of the material.

The thickness, density, specific heat, and ignition temperature used in the calculation of the ignition times are given in Table 3.2 [32]. It should be noted that if the thickness of a given material was unknown, it was approximated as 6 mm. The density and specific heat of the material are assumed to be independent of temperature for this calculation of ignition time.

Fig. 3.7 shows these ignition time predictions for several materials which have been grouped according to their accepted UL-94V rating [10]. Notice that none of the materials have an ignition time of less than 10 seconds. This result predicts that none of the materials will ignite during the first flame application. In fact, many of these materials do ignite, including some that sustain burning and allow the flame to spread. With this inaccuracy in mind, there exists a general pattern among the materials such that most V-0 materials have greater ignition times than V-2 and HB materials; perhaps indicating that a more detailed analysis might yield valuable results. Included in a more detailed analysis would be the edge and end effects associated with the UL-94V test. Work by Wang et al. [33], found that edge effects can reduce ignition times by nearly a factor of 3.

Table 3.2: Thickness, Density, Specific Heat, and Ignition Temperature

Polymer	Thickness (mm)	Density (kg/m^3)	Specifc Heat (kJ/kg-K)	Ignition Temperature (K)
PVC	6.1	1415	0.98	668
PAI	6	1420	1.0	799
ETFE	6	1700	1.0	813
PEEK	6	1310	1.7	843
PPS	6	1300	1.02	848
ECTF	6	1690	1.17	886
PTFE	6	2150	1.05	903
CPVC	6	1540	0.78	916
PC	6	1200	1.22	773
PMMA	5.35	1175	1.4	590
POM	6.75	1420	1.37	617
PS	6	1045	1.25	729
PP	6	880	1.88	640
UPT	6	1230	1.3	653
PBT	6	1350	1.61	655
ABS	6.35	1050	1.5	667
PET	6	1345	1.15	680
HIPS	6.14	1045	1.4	686
PA6	6	1130	1.55	705
PA66	6.73	1140	1.57	729
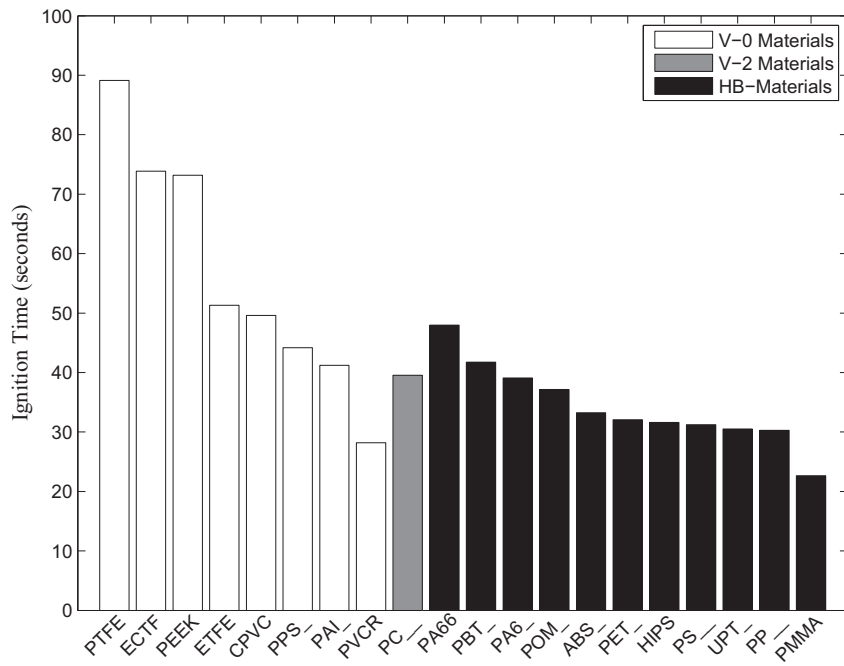
Figure 3.8: Ignition Times for Common Polymeric Materials ($\dot{q}'' = 60kW/m^2$)

Chapter 4

Sustained Burning

The following analysis does not rely on empirical correlations. Rather, the criteria for sustained burning was derived from a theory proposed by Quintiere [34], which predicts a critical mass flux at extinction. This mass flux value can be used to calculate a critical heat release rate for sustained burning. As was mentioned previously, this analysis proposes that the heat release rate for a burning polymeric material can be compared to critical heat release rates for sustained burning to predict material performance in the UL-94V Test.

4.1 Theoretical Basis for Predicting Sustained Burning

In his paper, *A Theoretical Basis for Flammability Properties*, Quintiere [34] suggests that the critical mass flux at extinction can be approximated by Eq. 4.1:

$$\dot{m}'' = \frac{(h_c/c_{p,air})Y_{ox,\infty}\Delta h_{ox}}{\Delta h_c[1 - (c_{p,air}(T_{f,crit} - T_\infty)/Y_{ox,\infty}\Delta h_{ox})]} \tag{4.1}$$

where the heat of combustion per unit mass of oxygen, Δh_{ox}, is 13.1 kJ/g per unit mass of oxygen, the critical flame temperature, T_f, is 1573 K, the specific heat of air is $1.0 \times 10^{-3}kJ/(g - K)$, and the mass fraction of oxygen in air, $Y_{ox,\infty}$ is 0.233.

The heat release rate at extinction, using this critical mass flux, is given by:

$$\dot{Q}'' = \dot{m}''\Delta h_c = (\frac{h_c}{c_{p,air}})\frac{Y_{ox,\infty}\Delta h_{ox}}{[1 - (c_{p,air}(T_{f,crit} - T_\infty)/Y_{ox,\infty}\Delta h_{ox})]} \tag{4.2}$$

where Δh_c is the heat of combustion of the fuel of interest and h_c is the convective heat transfer coefficient.

This approach for the critical mass flux in burning was first proposed by Roberts and Quince [35]. Their analysis was for liquid fuels while the one presented here is relevant to solid fuels.

4.2 Applying Theory to Develop Sustained Burning Criteria

In this section, the value of the convective heat transfer coefficient, h_c, is calculated. This convective heat transfer coefficient applies to the condition of the flame on the burning sample. A characteristic length of 10 mm was chosen because the 20 mm flame from the UL-94V test is positioned such that the first 10 mm of the sample is within the flame zone. The properties used in the following calculation were taken for air at $1000°C$ [37]:

$T_s = 1300°C$, $T_\infty = 1000°C$, $\beta = \frac{1}{T_\infty} = 0.000786 K^{-1}$, $k = 0.081 \frac{W}{m-K}$, $Pr = \frac{\nu}{\alpha} = 0.70$, $\nu = 1.8 \times 10^{-4} m^2/sec$, and $\alpha = 2.57 \times 10^{-4} m^2/sec$,

The Rayleigh Number was calculated using the following equation [38]:

$$Ra_L = Gr_L Pr = \frac{g\beta(T_s - T_\infty)L^3}{\nu\alpha} \tag{4.3}$$

The Nusselt Number correlation was taken from [38]:

$$Nu_L = \frac{\bar{h}L}{k} = 0.68 + \frac{0.670 Ra_L^{1/4}}{[1 + (0.492/Pr)^{9/16}]^{4/9}} \tag{4.4}$$

Now, one can calculate the time-average convective heat transfer coefficient for the condition of the flame on the burning sample:

$$\bar{h} = \frac{h}{L}(\bar{Nu}_L) = 20.6 \frac{W}{m-K} \tag{4.5}$$

Therefore, the critical heat release rate for sustained burning is:

$$\dot{Q}''_{crit,sustain} = 108 kW/m^2 \tag{4.6}$$

The heat release rate for flaming combustion for the materials of interest will be compared to this critical value in Section 7.3.

Chapter 5

Flame Spread

Provided that the specimen has ignited and burning is sustained, the flame spread on the specimen will ultimately determine the rating of the material for the UL-94V test. If afterflame or afterglow reaches the holding clamp, the material will fail the UL-94V test and the material will then be tested in accordance with the UL-94HB standard. As a result, determining the a criterion for flame spread on a sample is extremely important. In this section, a critical heat release rate for flame spread will be calculated based on correlations between flame height and heat release rate for wall flames along incombustible samples. The heat release rate for each of the materials can then be compared to this critical value to predict flame spread.

5.1 Theoretical Basis for Predicting Flame Spread

Quintiere [36] has provided an equation for wind-aided flame spread velocity on a thermally thin material. Heat transfer to the region downstream from the pyrolysis zone due to the buoyancy induced flow allows the flame to spread in the upward direction. Fig. 5.1 provides a simple description of the burn-out, pyrolysis, and convectively heated regions.

The velocity of the pyrolysis front is defined in Eq. 5.1 [36]:

$$V = \frac{\dot{q}''\Delta}{\rho c_p \delta (T_{ig} - T_s)} \tag{5.1}$$

where $\dot{q}''$ is the maximum heat flux at the pyrolysis front, Δ is the region of which the
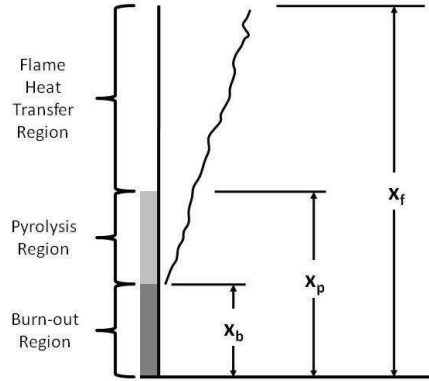
Figure 5.1: Diagram of A Vertical Burning Wall

heat transfer from the adjacent flames occurs, T_{ig} is the ignition temperature of the solid, and T_s is the initial temperature of the solid.

The author argues that the velocity of the burnout front can be derived from kinematic arguments by assuming that the front velocity is slowly varying in time. This assumption allows for the velocity of the pyrolysis front to be approximated as shown in Eq. 5.2:

$$V = \frac{dx_p}{dt} = \frac{x_p(t + t_{ig}) - x_p(t)}{t_{ig}} = \frac{x_f(t_{ig}) - x_p(t)}{t_{ig}} \tag{5.2}$$

where, x_p is position of the pyrolysis front.

As mentioned previously, the flame height above can be expressed in terms of the heat release rate per unit width of the sample as follows in Eq. 5.3:

$$x_f = C_f(\dot{Q}')^n \tag{5.3}$$

where C_f and n are empirically determined.

One can choose to express the heat release rate, $\dot{Q}$, in terms of the heat release rate per unit area, $\dot{Q}''$, pyrolysis position, x_p, and width of the sample, w, as follows in Eq. 5.4:

$$\dot{Q} = \dot{Q}'' x_p w \tag{5.4}$$

Then,

$$x_f = C_f \frac{(\dot{Q}'' x_p w)}{w} = C_f(\dot{Q}'' x_p)^n \tag{5.5}$$

When Eq. 5.5 is substituted into Eq. 5.2

$$\frac{dx_p}{dt} = \frac{(C_f \dot{Q}'' x_p)^n - x_p}{t_{ignition}} \tag{5.6}$$

In order for flame spread to occur, the time derivative of the position of the pyrolysis front must be greater than zero:

$$\frac{dx_p}{dt} > 0 \tag{5.7}$$

Therefore, for flame spread to occur, the following must be true:

$$(C_f \dot{Q}'' x_p)^n - x_p > 0 \tag{5.8}$$

To predict the flame spread along a specimen in UL-94V, empirical values for the relationship between the heat release rate per unit width of the burning specimen and the flame height were needed.

5.2 Measuring Flame Height and HRR for Burning Specimens

The following sections described the experiments and results used to develop the empirical relationships between flame height and heat release rate for burning polymeric materials tested in accordance with UL-94V.

5.2.1 Experiments

For these experiments, a specimen of standard length (125 mm) and width (13.0 mm) was cut from an incombustible material, with a thickness of approximately 6 mm. This thickness is considered to be representative of the materials tested as it falls within the the ranged prescribed by the standard. A burning material was simulated in one of two ways: (1) Applying a diffusion flame to the incombustible sample or (2) Wetting the incombustible sample with a liquid fuel. Calculation of the energy release rate varied for each method. The flame height measured was the average flame height around which the flame tip fluctuated. Some measure of consistency was achieved by having multiple observers conduct the same flame height measurement.

First, the Tirril Burner purchased from Humboldt Manufacturing, Inc., was used to produce a methane diffusion flame. A wing tip was fashioned from aluminum foil and attached to the burner tube. The wing tip was designed to fully surround the bottom edges of the sample. The resulting line burner was positioned so that the top of the wing tip was level with the bottom edge of the specimen, as shown in Fig. 5.2.

Proper positioning of the aluminum foil made it possible to simulate the burning behavior witnessed during the UL-94 Test; including equal flame heights on both faces of the specimen. The flow rate of methane gas was measured using the Omega FL-112 Rotameter. The height of the flames was measured visually and any variance between the front and back of the specimen, or fluctuation due to turbulent behavior, was noted.

The heat release rate was then calculated for each flow rate and flame height measurement using the following equation:

$$\dot{Q} = \Delta h_c \times \dot{m}_{fuel} \tag{5.9}$$
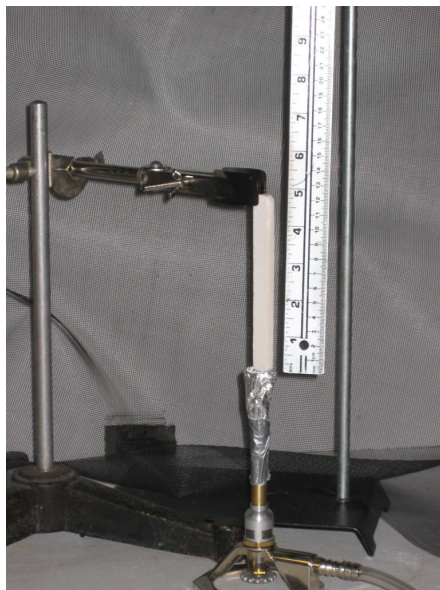
Figure 5.2: Line Burner used to Measure Flame Height vs. Heat Release Rate

where the heat of combustion, Δh_c, is 49.6 kJ/g for methane.

Additional measurements of flame height versus heat release rate were taken by burning heptane and methanol fuel that had been applied to the absorbent incombustible samples. Using the the burning rate of the fuel, the heat release rate could be calculated. Also, the height of the flames was measured as before.

The mass of the incombustible specimen was first measured using a digital scale before being mounted as in the UL-94V test. Next, a graduated cylinder containing a known amount of liquid fuel was moved into position and used to wet the mounted sample. The volume of the liquid fuel applied to the sample was recorded. While immersed in the liquid fuel, the length over which the fuel wetted the sample was also recorded; being careful to note the wick-like behavior of the material. The area over which the sample was wetted simulates the pyrolysis region. Following the removal of the graduated cylinder, the

sample was then immediately ignited before a significant volume of fuel could evaporate; simultaneously, measurement of the duration of the trial was started. As soon as the flame height was observed, the flame was extinguished and the time of the trial was recorded. The sample was then removed and the mass was measured again to determine the amount of fuel remaining on the sample.

The burning sample was not allowed to self extinguish because of the relationship between the mass burning rate and the mass of available fuel remaining. As the amount of fuel present on the sample decreases, the burning rate also decreases. Therefore, taking the time average burning rate over the entire trial would have yielded a low, and inaccurate, burning rate. By extinguishing the flame, a reasonably constant burning rate and thereby the heat release rate, was maintained for each trial.

Each one of these experiments yielded the initial mass of the specimen, m_o, the volume of fuel applied, $V_{applied}$, flame height, X_f, the final mass, m_{final}, and the time duration Δt. Calculation of the burning rate was done as follows:

$$\dot{m} = \frac{m_{final} - (m_o + \rho_{fuel} V_{applied})}{\Delta t} \tag{5.10}$$

where the $\rho_{methanol} = 0.791 g/mL$ and $\rho_{heptane} = 0.680 g/mL$.

Given the burning rate, the heat release rate was calculated using Eq. 5.9 where $\Delta h_c = 19.1 kJ/g$ for methanol and $\Delta h_c = 41.2 kJ/g$ for heptane.

5.2.2   Results

The minimum energy release rate for the heat flux measurements was 0.05 kW, corresponding to a minimum flow rate of 85.8 mL/min of methane gas. This yields a minimum energy release rate per unit width of 3 kW/m. The maximum energy release

rate for the heat flux measurements was 3 kW, corresponding to a maximum flow rate of 5500 mL/min of methane gas. This yields a maximum energy release rate per unit width of 200 kW/m.

For the methanol wetted samples, the minimum heat release rate per unit width measured was 9 kW/m, which corresponded to a flame height of 7 cm. The maximum heat release rate per unit width for methanol measured was 51 kW/m, which corresponded with a flame height of 28 cm. For the heptane wetted samples, the minimum heat release rate per unit area was 59 kW/m, which corresponded with a flame height of 31 cm. The maximum heat release rate per unit width for heptane measured was 114 kW/m, which corresponded with a flame height of 45 cm.

The resulting data points of heat release rate per unit width and flame height for both the premixed flames and the wetted samples are shown in Fig. 6.6. It should be noted that the values for wetted samples show good agreement with those of the premixed flame.

The above relationship between flame height and energy release rate per unit width can be expressed as follows in Eq. 5.11:

$$x_f = C_f(\frac{\dot{Q}}{w})^n \tag{5.11}$$

where $\dot{Q}$ is the heat release rate, w is the width of the sample, and C_f and n are empirical constants.

Fitting a curve to the data shown earlier in Fig. 5.3, for flame height versus energy release rate per unit width yields values 33.25 cm^2/kW and 1 for C_f and n respectively.

Similar to the analysis from Tewarson [26], the flame height over pyrolysis position (x_f/x_p) is plotted against the normalized chemical heat release rate (NCHRR) in Fig. 5.4 for the methanol and heptane wetted samples.
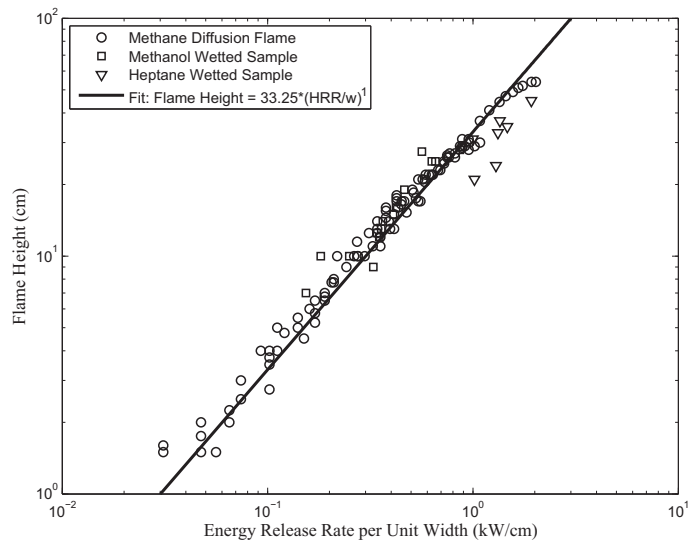
Figure 5.3: Flame Height vs. Heat Release Rate per Unit Width
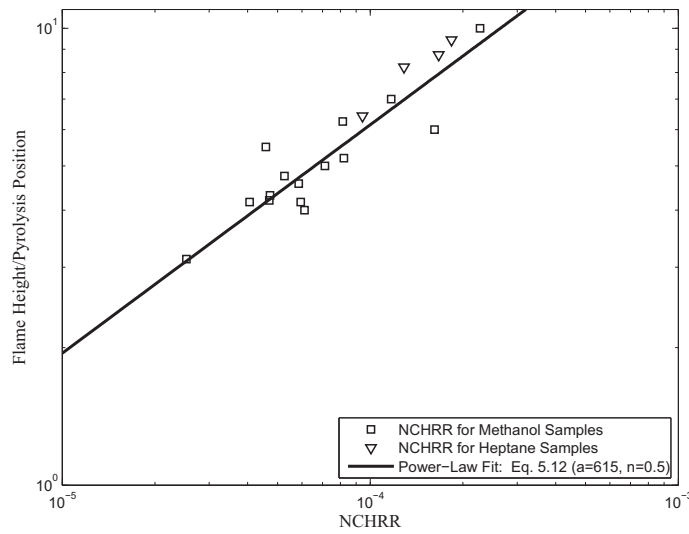
Figure 5.4: X_f/X_p vs. $NCHRR$ for Methanol and Heptane Wetted Samples

The ratio of flame height over pyrolysis position versus the normalized chemical energy heat release rate also follows a first-order relationship:

$$\frac{X_f}{X_p} = a[NCHRR]^n \tag{5.12}$$

The data collected here yields $a = 615$ and $n = 0.5$.

5.3 Developing Flame Spread Criterion

Because energy release rate per unit width follows a first order relationship with flame length as shown in Figure 5.3, it becomes much easier to predict the heat release rate criterion for flame spread as shown in Eq. 5.13:

$$\frac{dx_p}{dt} = \frac{x_p(C_f\dot{Q}'' - 1)}{t_{ignition}} \tag{5.13}$$

The criteria for flame spread given in Eq. 5.7 can now be re-written for $C_f = 33.25$ cm^2/kW:

$$\dot{Q}'' > \frac{1}{C_f} \tag{5.14}$$

$$\dot{Q}'' > \frac{1}{C_f} = \frac{1}{33.25cm^2/kW} = 300kW/m^2 \tag{5.15}$$

$$\dot{Q}''_{crit,flamespread} > 300kW/m^2 \tag{5.16}$$

The value for the heat release rate per unit area given in Eq 5.16 represents the critical heat release rate per unit area above which flame spread occurs for the UL-94V test. The heat release rate for flaming combustion for the materials of interest will be compared to this critical value for flame spread in Section 7.4.

Chapter 6

A Discussion of Melting Behavior

6.1   Objective

Because the presence of melting drips differentiates a V-1 material from a V-2, it is necessary to gain an improved understanding of the melting behavior of the specimens being tested (See Table 1.1). Predicting the melt behavior of the materials is essential to any complete understanding of the phenomena governing the results of the test. The following analysis is proposed.

Fig. 6.1 shows an arbitrary region, defined as the *Melt Region*, which has reached the melting temperature of the material. By applying the conservation of momentum equation in the x-direction, one can find an expression for the velocity of the melt flow.

6.2   Analysis

The Conservation of Momentum equation (X-Direction) is written as:

$$\rho(u\frac{\partial u}{\partial x} + v\frac{\partial u}{\partial y}) = \mu_{melt}\frac{\partial^2 u}{\partial y^2} - \frac{\partial p}{\partial x} + \rho_{melt}g \qquad (6.1)$$

where μ_{melt} and ρ_{melt} are the viscosity and density of the melted material, respectively.

Assuming that velocity, u, is a function of y only $(u \neq u(x))$ and $\frac{\partial u}{\partial x} = -\rho_\infty g = 0$, the momentum equation can be expressed as an Ordinary Differential Equation:

$$\frac{d^2u}{dy^2} = \frac{-\rho_{melt}g}{\mu_{melt}} \qquad (6.2)$$

50
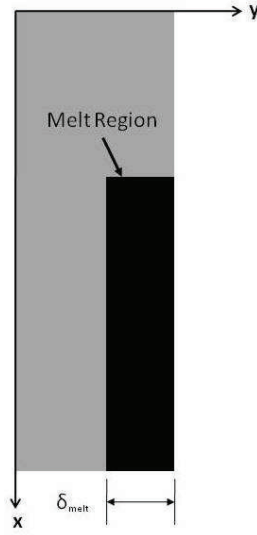
Figure 6.1: Diagram of Melt Region

The boundary conditions are:

$$at \ y = \delta_{melt}, \frac{du}{dy} = 0 \qquad (6.3)$$

$$at \ y = 0, u = 0 \qquad (6.4)$$

Solving for the velocity, u, by integration and applying the boundary conditions, yields:

$$u = \frac{\rho_{melt} g}{\mu_{melt}} y(\delta_{melt} - \frac{y}{2}) \qquad (6.5)$$

Using this expression for the velocity of the melt, one can predict the flow rate of the melted material provided that the melt thickness is known. This melt thickness is a function of the heating rate. The first step in calculating the flow rate of the material is to define the net incident heat flux to the material (Eq. 6.6):

$$\dot{q}''_{net} = \dot{q}''_{incident} - \sigma(T^4_{melt} - T^4_o) \qquad (6.6)$$

51

where T_{melt} is the melting temperature of the material, T_o is the initial temperature of the material, and σ is the *Stefan-Boltzmann Constant.*

The growth of the thickness of the melted material, δ_{melt}, is dependent on the net incident heat flux, $(\dot{q}''_{net})$, the density of the melted material, (ρ_{melt}), and the heat of melting, (Δh_{melt}). By assuming no heat loss to the solid material:

$$\dot{q}''_{net} = \rho_{melt} \frac{d\delta_{melt}}{dt} \Delta h_{melt} \qquad (6.7)$$

The heat of melting of a material can be measured using Differential Scanning Calorimetry (DSC), as described by Kim and Quintiere [39]. By subjecting the substance being tested and a reference material to a controlled temperature program, one can measure the difference in energy inputs to both the substance and reference material as a function of temperature. DSC allows the determination of heat capacity, transition temperature, and the associated change in energy [39]. Also, a study by Stoliarov and Walters [40] proposed that DSC be used to determine the heats of gasification of common polymers.

Solving for the melt thickness, δ_m:

$$\delta_{melt} = \frac{\dot{q}''_{net} - \sigma(T^4_{melt} - T^4_o)}{\rho_{melt} \Delta h_{melt}} (t - t_{melt}) \qquad (6.8)$$

where t is the total time elapsed after application of the incident heat flux, and t_{melt} is the time at which the onset of melting occurs.

With these expressions for velocity (Eq. 6.5) and melt thickness (Eq. 6.8), one can find an expression for the mass flow rate of the melt region in terms of ρ_{melt}, μ_{melt}, δ_{melt} as follows:

$$\dot{m} = \frac{w \rho^2_{melt} g}{\mu_{melt}} \frac{\delta_{melt}}{3} \qquad (6.9)$$

Unfortunately, the density and viscosity of the melted polymeric materials are not

52

readily available. Limited work by Ohlmeiller and Shields [41] includes measurement of the melt viscosity as a function of temperature for Nylon 66, Polystyrene, Polypropylene, and PMMA.

6.3   Summary

The above analysis uses first principles to predict both the onset of melting and the mass flow rate of the melted material. Given the appropriate material properties, it is possible that the melting behavior of polymeric materials can be predicted.

Chapter 7

Applying Theoretical Criteria to Predict Test Results

The experiments and analysis presented here have established criteria for igni-

tion, sustained burning, and flame spread in terms of the heat release rate of plastic

materials tested in accordance with UL-94V. This chapter includes a discussion of

the assumptions and calculations that were made in determining the heat release

rate for common plastic materials. The heat release rates of these materials is de-

pendent on the material property known as the Heat Release Parameter, HRP. The

heat release rate of the materials of interest can then be compared to the established

criteria.

7.1   Calculating Heat Release Rate for Common Polymers

The following section describes the calculation of the heat release rate of the

plastic materials of interest. These heat release rate values can then be compared

to the critical heat release rate values for sustained burning and flame spread. The

calculation of this heat release rate per unit area for each of the UL-94V materials

was calculated as follows in Eq. 7.1:

$$\dot{Q}'' = \dot{q}''_{net,incident} \times HRP \tag{7.1}$$

where $\dot{Q}''$ is the heat release rate per unit area, $\dot{q}''_{net,incident}$ is the total incident

heat flux per unit area, and HRP is the heat release parameter of the material in

question.

The steady burning rate for a fluid is given by Eq. 7.2:

$$\dot{m}'' = \frac{\dot{q}''_{net,incident}}{L} \tag{7.2}$$

Given,

$$HRP = \frac{\Delta h_c}{L} \tag{7.3}$$

The heat release rate per unit area in terms of the burning rate

$$\dot{Q}'' = \dot{m}'' \times \Delta h_c \tag{7.4}$$

becomes

$$\dot{Q}'' = \dot{q}''_{net,incident} \times HRP \tag{7.5}$$

Application of the HRP in Eq. 7.5 assumes that the burning rate of the material is steady. This assumption results in a conservative estimate in that it overestimates the heat release rate of the material.

The net incident heat flux is the sum of the incident heat flux in the flame zone and the losses to the surrounding environment as shown below:

$$\dot{q}''_{net,incident} = \dot{q}''_{flamezone} - CHF \tag{7.6}$$

$$CHF = \epsilon\sigma(T_{ig}^4 - T_\infty^4) \tag{7.7}$$

Blackbody radiation ($\epsilon = 1$) is assumed.

In summary, the heat release rate per unit area for each of the UL-94V materials can be calculated as follows in Eq. 7.8:

$$\dot{Q}'' = (\dot{q}''_{flamezone} - \epsilon\sigma(T_{ig}^4 - T_\infty^4)) \times HRP \tag{7.8}$$

55

Table 7.1: HRP Values and Ignition Temperatures of Common Polymers[10]

Polymer	HRP	Ignition Temperature (K)
Polyvinyl Chloride (PVC-Rigid)	3	916
Polyamideimide (PAI)	4	799
Polyethylenetetrafluoroethylene (ETFE)	6	813
Polyetheretherketone (PEEK)	6	843
Poly-1,4-phenylenesulfide (PPS)	4	848
(ECTFE)	3	886
Polytetrafluoroethylene (PTFE)	2	903
(CPVC)	2	916
Polyvinyl Chloride (PVC-Flexibile)	5	591
Polycarbonate (PC)	9	773
Poly(methyl methacrylate) (PMMA)	14	590
Polyoxymethylene (POM)	6	617
Polystyrene (PS)	16	629
Polypropylene (PP)	22	640
(UPT)	8	653
Polybutyleneterephthalate (PBT)	16	655
Acrylonitrile butadiene styrene (ABS)	13	667
(PET)	13	680
High-Impact Polystyrene (HIPS)	14	686
Polycaprolactam (PA6)	20	705
Polyamide 6,6 (PA66)	13	729

where T_{ig} and HRP are material properties. The HRP and T_{ig} for several common polymers are given in Table 7.1 [10].

At this time, it becomes necessary to measure the incident heat flux in the flame zone, $\dot{q}''_{flamezone}$.

7.2   Measuring Heat Flux for Burning Specimens

The net incident heat flux in the flame zone of a burning material is needed to calculate the heat release rate of the plastic materials. This section describes the experiments used to quantify this incident heat flux.

7.2.1   Experiments

In these experiments, a specimen of standard length (125 mm) and width (13.0 mm) was cut from an incombustible material. The thickness of this inert specimen was approximately 6 mm and was considered to be representative of the materials tested as it falls within the prescribed range and also can be considered thermally thin.

A wing tip was fashioned from aluminum foil and attached to the diffusion flame burner tube of the Tirrill Burner. The width of the wing tip is equal to the width of a standard specimen (approximately 1.5 cm). The resulting line burner was positioned so that the top of the wing tip was level with the bottom edge of the specimen, as shown in Fig. 7.1. Further, the wing tip was arranged such that the flame was present along the front of the material only. The flame behavior would likely have been changed by the protrusion of the heat flux gauge on back of the
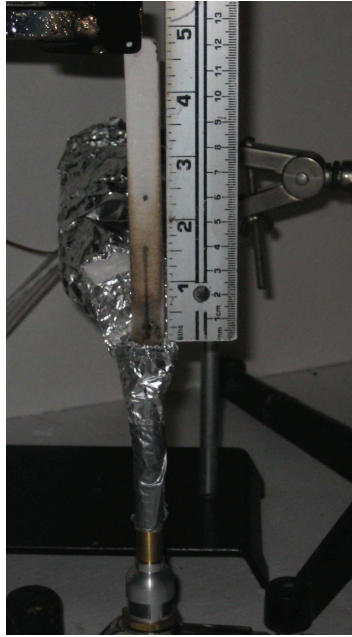
Figure 7.1: Heat Flux Measurements along Vertical Centerline of Sample

specimen itself if the flame had been present on both sides.

The incident heat flux from the flame to the specimen was measured using the 1/8 inch diameter water-cooled heat flux gauge. The face of the gauge was positioned such that it was flush with the front face of the incombustible specimen. Using a NETDAQ data acquisition system, the voltage difference was measured at 0.01 s intervals for a 30 s trial. This data was recorded in a Microsoft Excel Spreadsheet where the average and maximum values for the incident heat flux to the surface could be calculated for each experiment.

The flow of rate methane gas used in these experiments was measured using the Omega FL-112 Rotameter and the stainless steel float. The flame height was measured visually against a meter stick. The flame height recorded was the average flame height around which the flame tip fluctuated. Some measure of consistency in measuring this

fluctuating flame height was achieved by having multiple observers conduct the same flame height measurement.

7.2.2 Results

The minimum energy release rate for the heat flux measurements was 0.02 kW, corresponding to a minimum flow rate of 43.7 mL/min of methane gas. This yielded a minimum energy release rate per unit width of 1.33 kW/m. The maximum energy release rate for the heat flux measurements was 3 kW, corresponding to a maximum flow rate of 5590 mL/min of methane gas. This yielded a maximum energy release rate per unit width of 200 kW/m.

Similar to other studies presented by Lattimer [14] , the resulting data were plotted as heat flux versus position of the heat flux gauge over flame height (X/X_f) on a log-log scale. Although there is some scatter in the data, this presentation method tends to collapse the data in such a way that power-law correlations can be found.

The turbulent nature of the flame at the higher flame heights $(X_f > 7cm)$ necessitated that both the maximum heat flux recorded and the average heat flux over the interval be presented. In Fig. 7.2, the maximum heat flux value for each 30 s trial is plotted. In Fig. 7.3, the time-average heat flux values for each 30 s trial are plotted.

Lines of best fit were added to the plots of maximum and average heat flux per unit area versus X/X_f to appropriately characterize the results. These equations conservatively bound the data in the power-law growth, constant, and power-law decay regions of the plot.

For the Maximum Heat Flux (Fig. 7.2):

$$\dot{q}'' = 214(X/X_f)^{1.3} \text{ kW/m}^2 \text{ for } (X/X_f) \leq 0.4 \tag{7.9}$$
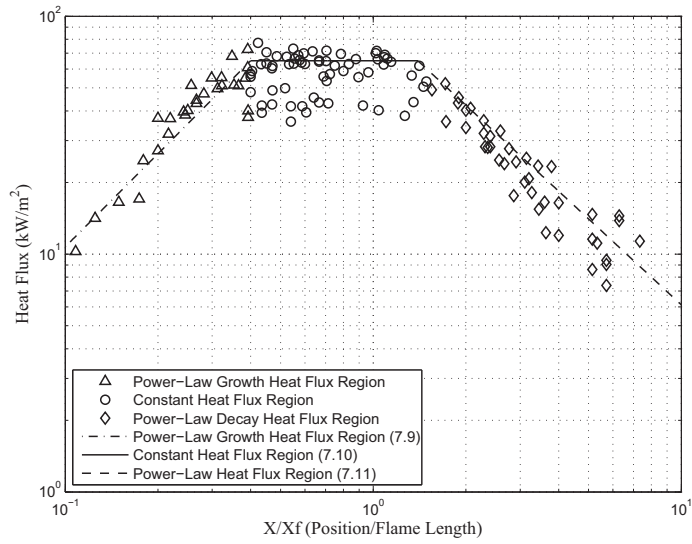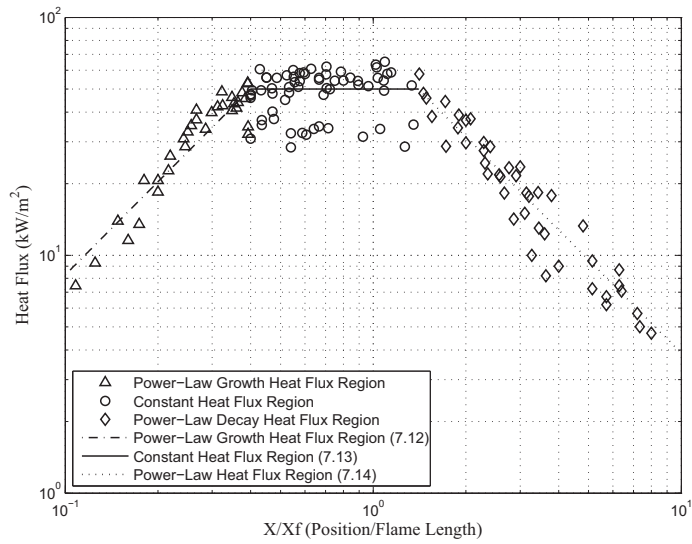
Figure 7.2: Maximum Heat Flux for Burning UL-94V Specimens

Figure 7.3: Average Heat Flux for Burning UL-94V Specimens

$$\dot{q}'' = 65 \text{ kW/m}^2 \text{ for } 0.4 \ < \ (X/X_f) \leq 1.4 \tag{7.10}$$

$$\dot{q}'' = 97(X/X_f)^{-1.2} \text{ kW}/m^2 \text{ for } (X/X_f) > 1.4 \tag{7.11}$$

For the Average Heat Flux (Fig. 7.3):

$$\dot{q}'' = 165(X/X_f)^{1.3} \text{ kW}/m^2 \text{ for } (X/X_f) \leq 0.4 \tag{7.12}$$

$$\dot{q}'' = 50 \text{ kW}/m^2 \text{ for } 0.4 \ < \ (X/X_f) \leq 1.4 \tag{7.13}$$

$$\dot{q}'' = 77.5(X/X_f)^{-1.3} \text{ kW}/m^2 \text{ for } (X/X_f) > 1.4 \tag{7.14}$$

In summary, the heat flux per unit area was characterized along the height of the sample. Lines of best fit that appropriately characterize the data were found. The constant incident heat flux measured in the flame zone of 65 kW/m^2 can now be used to estimate the heat release rate of the burning polymeric materials.

7.3   Applying Sustained Burning Criteria

Applying the sustained burning criteria is relatively simple, in that it requires only a comparison of the heat release rate of the burning material calculated in Section 7.2 to the critical heat release rate required for sustained burning found in Chapter 4 ($\dot{Q}''_{crit,sustain}$=108 kW/m^2). Presentation of these results is done graphically in Fig. 7.4.

It is important to remember that V-0 rated materials do not sustain burning, while V-2 and HB materials do. Therefore, the heat release rate of all V-0 materials should theoretically be less than 108 kW/m^2, while the heat release rate of all V-2 and HB materials should be greater than 108 kW/m^2. However, the critical heat release criteria found for sustained burning does not completely describe the demarcation between V-0 and V-1/V-2 materials. In fact, some plastic materials such as PEEK, PPS, and ECTFE,
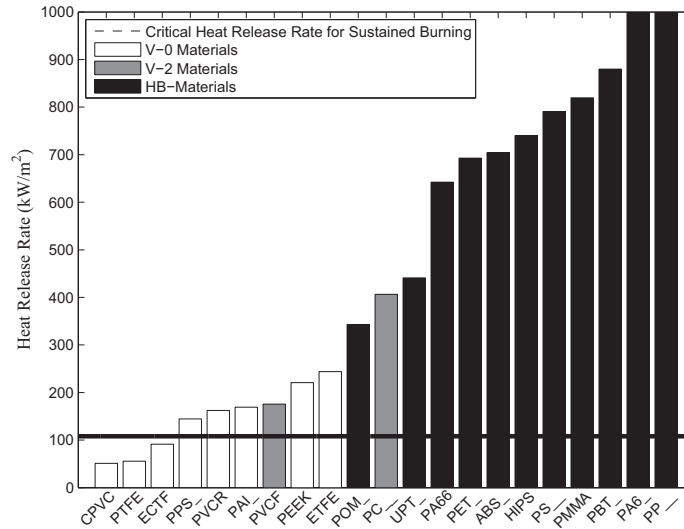
Figure 7.4: Critical Heat Release for Sustained Burning

which are commonly accepted as V-0 materials that do not sustain burning, have heat release rates of greater than 108 kW/m^2. This discrepancy is likely due to the assumption of steady burning of the materials which overestimates the heat release rate of the burning material.

7.4 Applying Flame Spread Criteria

The heat release rate of the material must be compared to the critical heat release rate required for flame spread. Presentation of these results is done graphically in Fig. 7.5.

It is important to remember that in order to be classified as a V-Rated material, the flame cannot spread all the way to the holding clamp. If the material allows the flame to spread up to the clamp, the material fails the UL-94V test and then must be tested
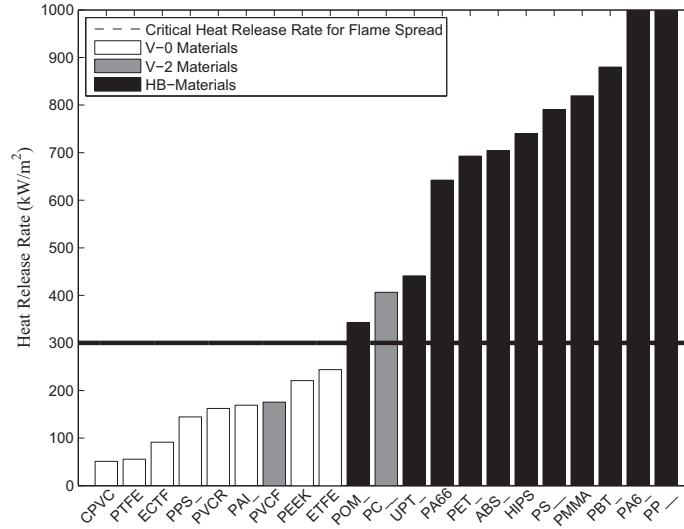
Figure 7.5: Critical Heat Release for FlameSpread

in accordance with the UL-94HB test. The critical heat release criteria found for flame spread accounts in part for the demarcation between V-Rated and HB materials. For example, the heat release rate of Polycarbonate (PC) ($\dot{Q}'' = 452$ kW/m^2), is greater than $\dot{Q}''_{crit,flamespread}$. In reality, PC does not allow the flame to spread to the holding clamp and thereby passes the UL-94V test. This discrepancy is likely due to the assumption of steady burning of the materials, which overestimates the heat release rate of the burning material.

7.5   Predicting the Results of the UL-94V Test

In Chapter 1, the intrinsic heat release rates of some plastic materials [10] were compared by Lyon to the accepted UL-94 ratings of these materials. These same materials can be classified according to the sustained burning and flame spread criteria established

Table 7.2: Comparison of Results to Accepted Ratings [10]

Material	HRR (kW/m^2)	Predicted Rating	HRR_o (kW/m^2)	Accepted Rating
CPVC	61	V-0	-34±9	V-0
PTFE	65.4	V-0	-84±9	V-0
ECTF	106.4	V-0	-127±6	V-0
PPS	164.4	V-1 or V-2	-147±30	V-0
PVCR	177.4	V-1 or V-2	9±25	V-0
PAI	189.2	V-1 or V-2	-64±16	V-0
PVCF	190.5	V-1 or V-2	-91±19	V-2
PEEK	250.7	V-1 or V-2	-94±20	V-0
ETFE	273.9	V-1 or V-2	44±31	V-0
POM	373.2	HB	162±30	HB
PC	451.6	HB	89±32	V-2
UPT	480.9	HB	261±105	HB
PA66	707.3	HB	240±59	HB
PET	757.8	HB	424±168	HB
ABS	769.5	HB	359±66	HB
HIPS	810.1	HB	510±77	HB
PS	870.5	HB	410±66	HB
PMMA	889.7	HB	217±47	HB
PBT	959.7	HB	341±106	HB
PA6	1128.2	HB	187±55	HB
PP	1339.9	HB	369±79	HB

here. The UL-94 rating predicted here from the sustained burning and flame spread criteria can then be compared to both the accepted rating [10] and the intrinsic heat release rate criteria. Table 7.2 lists the materials in order of increasing heat release rate as calculated in Section 7.2, the predicted UL-94 rating, the intrinsic heat release rate, and the *Accepted Rating*. (The calculation of the HRR assumes $\dot{q}''_{net}$=70 kW/m^2.)

For the purposes of this analysis, materials that that do no sustain burning are classified as V-0 materials. Further, the criteria developed here do not allow one to differentiate between V-1 and V-2 materials because the ignition of the cotton by

flaming drops has not been addressed (See Table 1.1).

The most striking result is the demarcation between V-rated and HB-rated materials as predicted by the flame spread criteria. Except for Polycarbonate, all of the materials considered with an *Accepted Rating* of HB have a heat release rate of greater than 300 kW/m^2.

7.6   Comparison of Accepted Ratings to Physical Parameters

It is also possible to describe these results as they relate to certain material properties. After defining a Thermal Response Parameter for Thin Materials, TRP_{thin}, one can analyze the Accepted Ratings of these materials in terms of their HRP and TRP_{thin}.

$$TRP_{thin} = \rho c_p \delta (T_{ig} - T_o) \tag{7.15}$$

Materials which fail the UL-94V test tend to HRP values of greater than 6. It should be noted that V-2 materials shown in this plot do not follow the behavior that was just described. It is possible that the melting behavior of these materials causes the application of this HRP criterion to fail. It is difficult to definitively determine a criterion for the UL-94V test in terms of TRP_{thin} due to the limited data available, although it does appear that materials that fail the UL-94V test tend to have TRP_{thin}¡ 2600 kJ/m^2.
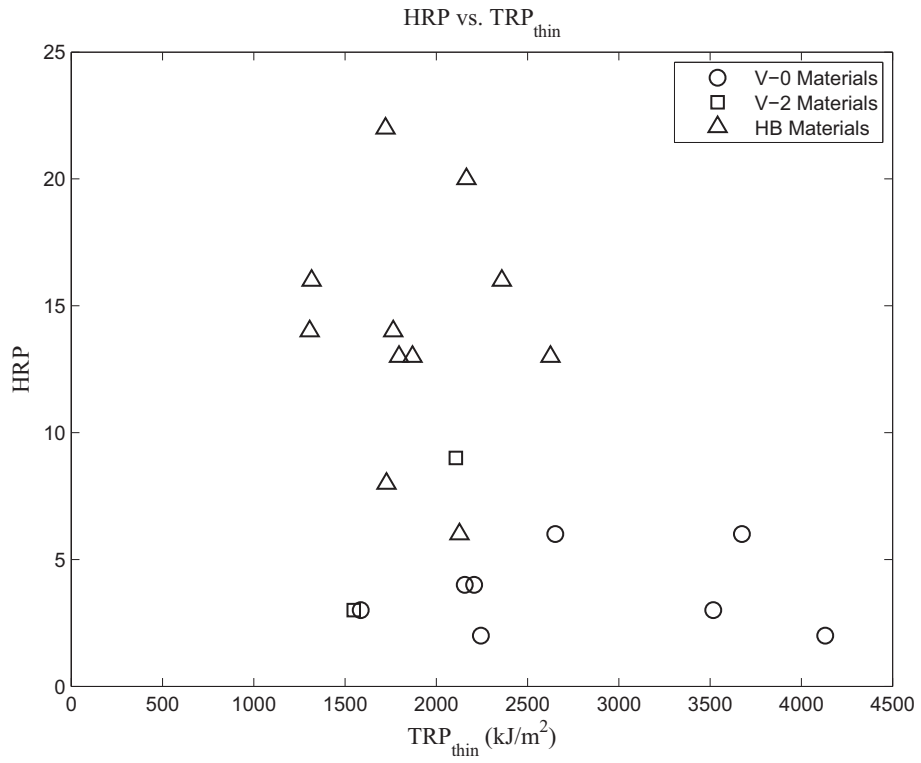
Figure 7.6: HRP vs. TRP_{thin}

Chapter 8

Conclusions

The UL-94 Flammability Test is one of the available pre-selection test programs conducted on plastic materials to measure flammability characteristics. This test determines the tendency of a material either to extinguish or to spread a flame, presuming that the specimen has been ignited by an applied pilot flame. This study focused on the UL-94V: Vertical Burning Test.

The ignition of the plastic materials was modeled using the thermally-thin approximation. Then a non-linear prediction of the ignition time for each of the materials when exposed to an incident heat flux was made. This incident heat flux was characterized for the setup given in the standard and then compared to measurements influenced by human factors, including flame height, distance from the burner to the specimen, and orientation angle of the burner. Although a general pattern exists among the materials such that V-0 materials have the longest ignition times, a more detailed analysis of the ignition process is needed to accurately predict this portion of the test.

In an effort to establish heat release rate criteria that could be used to predict sustained burning and flame spread, correlations between heat release rate, flame height, and heat flux to the plastic specimens were found.

By assuming that the burning rate of the plastic materials was steady, the Heat Release Parameter, HRP, could be used to calculate the heat release rate of the burning materials. This heat release rate for the each of the materials could then be compared to the sustained burning and flame spread criteria to predict the performance of the material.

The sustained burning and flame spread criteria were able to predict the performance of some of the plastic materials. The development of a more accurate burning model that does not assume steady burning and includes parameters such as edge effects, could allow for a more accurate calculation of the heat release rate of the burning materials and thus a more complete understanding of the UL-94V Flammability Test.

Appendix A

Engineering Drawing of UL-94V Standard Sample

Date March 11, 2009	Brian Downey
UL94V-Sample	Dimensions in Millimeters
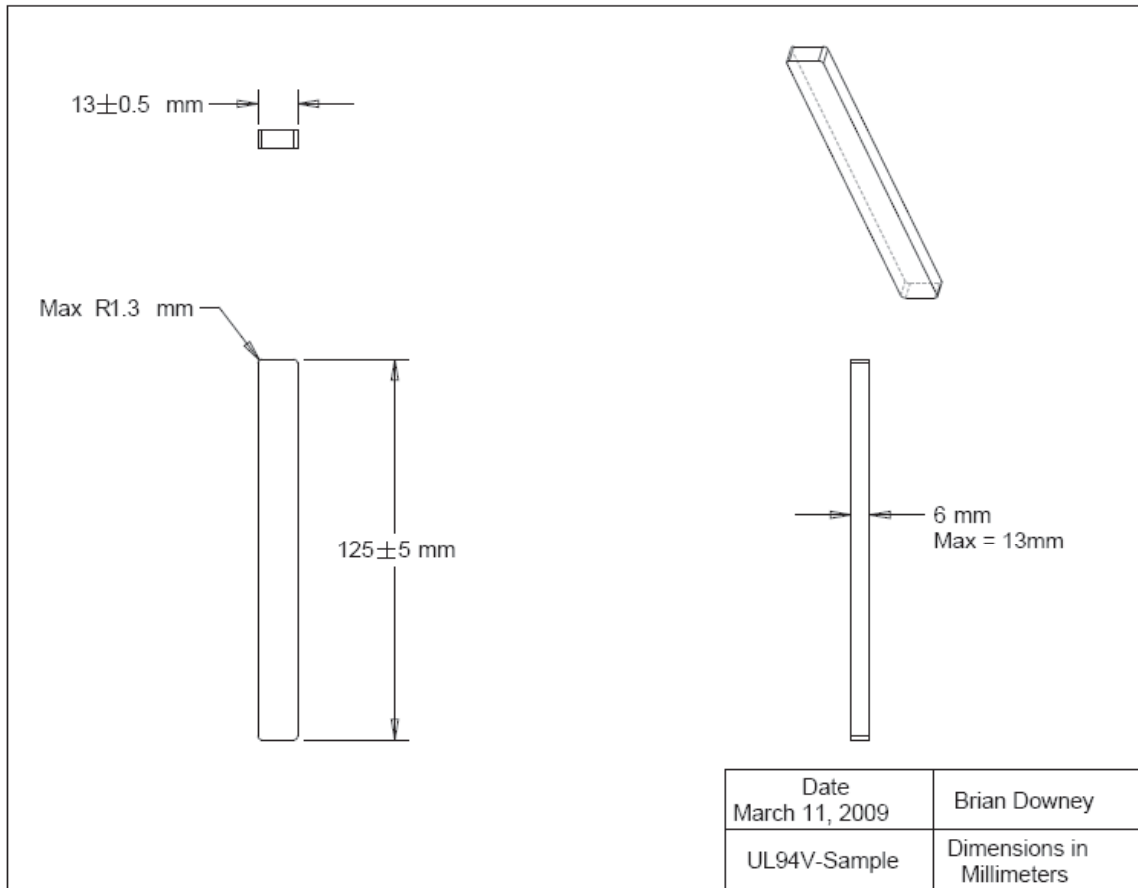
Appendix B

FL-110 Rotameter Correlated Flow Table

Correlated Flow Table

Tube Size 0		Fluid Methane	
Float Type Glass & Stainless Steel		Density 0.0006569 g/ml	
Serial No.		Viscosity 0.010919 cp	
Date 07-30-2008		Volume corrected to standard conditions Measured & flowing at 1 atm and 70 °F	

FLOW ml/min Glass	SCALE	FLOW ml/min S.S.	FLOW ml/min Glass	SCALE	FLOW ml/min S.S.	FLOW ml/min Glass	SCALE	FLOW ml/min S.S.	FLOW ml/min Glass	SCALE	FLOW ml/min S.S.
1.78	1	5.64	10.7	26	35.3	37.7	51	103	88.5	76	213
1.94	2	6.14	11.4	27	37.3	39.2	52	107	91.0	77	218
2.10	3	6.67	12.1	28	39.3	40.7	53	110	93.6	78	224
2.28	4	7.24	12.8	29	41.4	42.2	54	114	96.2	79	230
2.48	5	7.85	13.6	30	43.6	43.8	55	118	98.8	80	235
2.68	6	8.50	14.4	31	45.8	45.5	56	121	101	81	241
2.90	7	9.19	15.4	32	48.0	47.1	57	125	104	82	247
3.13	8	9.9	16.3	33	50.3	48.9	58	129	107	83	253
3.38	9	10.7	17.3	34	52.7	50.6	59	133	110	84	259
3.64	10	11.6	18.3	35	55.1	52.5	60	137	112	85	265
3.92	11	12.4	19.3	36	57.6	54.3	61	141	115	86	272
4.22	12	13.4	20.4	37	60.1	56.3	62	145	118	87	278
4.54	13	14.4	21.5	38	62.7	58.3	63	149	121	88	284
4.87	14	15.5	22.6	39	65.4	60.4	64	153	124	89	291
5.23	15	16.6	23.7	40	68.2	62.6	65	158	126	90	297
5.60	16	17.8	24.8	41	71.1	64.8	66	162	129	91	304
6.00	17	19.3	26.0	42	74.0	67.0	67	166	132	92	311
6.42	18	20.9	27.2	43	77.0	69.2	68	171	135	93	317
6.87	19	22.5	28.4	44	80.1	71.5	69	176	138	94	324
7.34	20	24.2	29.7	45	83.2	73.9	70	181	141	95	331
7.83	21	25.9	30.9	46	86.4	76.2	71	186	145	96	338
8.35	22	27.7	32.2	47	89.7	78.6	72	191	148	97	344
8.90	23	29.5	33.6	48	93.0	81.0	73	197	151	98	351
9.48	24	31.4	34.9	49	96.3	83.5	74	202	154	99	358
10.1	25	33.3	36.3	50	99.7	86.0	75	207	157	100	365

Appendix B

FL-112 Rotameter Correlated Flow Table

Correlated Flow Table

Tube Size 2

Float Type Glass & Stainless Steel

Serial No.

Date 07-14-2008

Fluid Methane

Density 0.0006569 g/ml

Viscosity 0.010919 cp

Volume corrected to standard conditions
Measured & flowing at 1 atm and 70 °F

FLOW ml/min Glass	SCALE	FLOW ml/min S.S.	FLOW ml/min Glass	SCALE	FLOW ml/min S.S.	FLOW ml/min Glass	SCALE	FLOW ml/min S.S.	FLOW ml/min Glass	SCALE	FLOW ml/min S.S.
8.60	1	27.3	552	26	1183	1349	51	2722	2298	76	4393
13.8	2	43.7	580	27	1237	1385	52	2788	2335	77	4460
20.5	3	65.1	607	28	1291	1421	53	2854	2373	78	4527
28.9	4	93.9	638	29	1345	1458	54	2921	2410	79	4594
39.1	5	131	668	30	1400	1496	55	2987	2448	80	4661
51.1	6	174	699	31	1455	1533	56	3054	2485	81	4728
65.6	7	219	729	32	1511	1572	57	3120	2522	82	4795
85.8	8	266	760	33	1568	1611	58	3187	2559	83	4861
108	9	313	790	34	1625	1649	59	3254	2596	84	4928
131	10	360	821	35	1683	1688	60	3321	2633	85	4995
155	11	408	852	36	1742	1726	61	3387	2669	86	5061
180	12	456	883	37	1805	1765	62	3454	2706	87	5128
205	13	505	915	38	1870	1803	63	3521	2742	88	5194
230	14	554	946	39	1935	1841	64	3588	2779	89	5260
256	15	603	978	40	2000	1880	65	3655	2815	90	5327
282	16	652	1010	41	2065	1918	66	3722	2851	91	5393
308	17	702	1042	42	2130	1956	67	3789	2887	92	5458
334	18	753	1075	43	2196	1994	68	3856	2923	93	5524
361	19	807	1108	44	2261	2033	69	3923	2958	94	5590
388	20	861	1141	45	2327	2071	70	3991	2994	95	5655
415	21	915	1175	46	2392	2109	71	4058	3029	96	5721
442	22	968	1209	47	2458	2147	72	4125	3064	97	5786
470	23	1022	1243	48	2524	2184	73	4192	3099	98	5851
497	24	1076	1278	49	2590	2222	74	4259	3134	99	5916
524	25	1129	1313	50	2656	2260	75	4326	3169	100	5981

Appendix C

Verification of Roper's Analysis for Diffusion Flames

Roper's analysis allows one to estimate the length of a diffusion flame produced by a circular port burner. The length of the flame is dependent on the flow rate and properties of the fuel, including the temperature (in K) and molar stoichiometric oxidizer to fuel ratio. For methane ($C_x H_y = CH_4$), this fuel ratio is:

$$S = 4.76(x + y/4) = 9.52 \tag{C.1}$$

The flame length given by Roper:

$$L_{flame} = 1330 \frac{Q_F (T_\infty / T_F)}{\ln 1 + 1/S} \tag{C.2}$$

where Q_F is the flow rate of the fuel in m^3/s, L_{flame} is the length of the diffusion flame in m, and T_∞ is the ambient temperature in K. For the purposes of this verification, the temperature of the fuel stream is equal to the ambient temperature.

Table C.1 and Table C.2 summarize the flame length prediction for several different flow rates and the flame length measured at that flow rate. The following plot graphically displays the measurements for comparison to the predicted values.
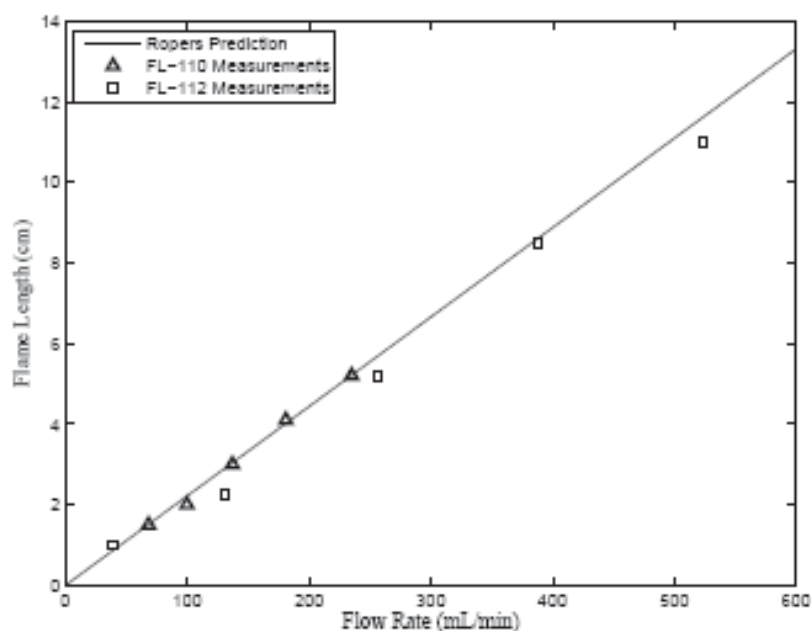
Figure C.1: Comparing Roper Prediction with Measured Values

Table C.1: Roper Correlation for FL-112 with Glass Float.

Division Marking	Flow Rate mL/min	Flame Length Prediction (cm)	Measured Flame Length (cm)
5	39.1	0.87	1
10	131	2.91	2.25
15	256	5.68	5.2
20	388	8.61	8.5
25	524	11.63	11

Table C.2: Roper Correlation for FL-110 with Stainless Steel Float

Division Marking	Flow Rate mL/min	Flame Length Prediction (cm)	Measured Flame Length (cm)
40	68.2	1.51	1.5
50	99.7	2.21	2
60	137	3.04	3
70	181	4.02	4.1
80	235	5.22	5.2

73

Bibliography

[1] UL-94: *Tests for Flammability of Plastic Materials for Parts in Devices and Appliances* (1996), Chicago, IL, USA: Underwriter's Laboratories.

[2] ASTM D5025: *Standard Specification for Laboratory Burner Used for Small-Scale Burning Tests on Plastic Materials* (2005), West Conshohocken, PA, USA: American Society for Testing and Materials.

[3] ASTM D5207: *Standard Practice for Confirmation of 20 mm (50 W) and 125 mm (500 W) Test Flames for Small Scale Burning sTests of Plastic Master-ils* (2003), West Conshohocken, PA, USA: American Society for Testing and Materials.

[4] Babrauskas, V., "Ignition: A Century of Research and an Assessment of Our Current Status," *Journal of Fire Protection Engineering*, 17, 3, pp. 165-183 (August 2007).

[5] Morgan, A. and M. Bundy, "Cone Calorimeter Analysis of UL-94V Rated Plastics," *Fire and Materials*, 31, pp. 257-283 (2007).

[6] Hong, S., J. Yang, S. Ahn, Y. Mun, and G. Lee, "Flame Retardancy of Various UL-94 Classified Materials Exposed to External Ignition Sources," *Fire and Materials*, 28, pp. 25-31 (2007).

[7] Schartel, B. and U. Braun. "Comprehensive Fire Behavior Assessment of Polymeric Materials Based on Cone Calorimeter Investigations," *e-Polymers*, 1, pp. 1-14 (January 2008).

[8] Bundy, M. and T. Ohlmeiller, "Bench Scale Flammability Measures for Electronic Equipment," *NISTIR 7031*, July 16, 2003.

[9] Lyon, R., N. Safronava, R. Walters, S. Stoliarov, "A Statistical Model for the Results of Flammability Tests," *Fire and Materials - Proceedings of the Eleventh International Conference*, Interscience Communications, London, UK, pp. 141-153 (2009).

[10] Lyon, R., "Plastics and Rubber," *Handbook of Building Materials for Fire Protection*, Chapter 3, McGraw-Hill, New York, NY, USA (2004).

[11] Tewarson, A. and S. Ogden, "Flame Behavior of Polymethylmethacrylate," *(*Combustion and Flame), 89, pp. 273-295 (1992).

[12] Fernandez-Pello, A. and T. Hirano, "Controlling Mechanisms of Flame Spread," *Combustion Science and Technology*, 32, 1, pp. 1-32 (1983).

[13] Alpert, R., "Pressure Modeling of Fire Controlled by Radiation," *Sixteenth Symposium on (International) On Combustion*, The Combustion Institute, Pittsburgh, PA, 1489.

[14] Lattimer, B.Y., "Heat Fluxes from Fires to Surfaces", *3rd Edition of SFPE Handbook of Fire Protection Engineering*, Section 2, Chapter 14, National Fire Protection Association, Quincy, MA, USA (2002).

[15] Hasemi, Y., "Thermal Modeling of Upward Flame Spread," in *Fire Safety Science-Proceedings of the First International Symposium*, International Association for Fire Safety Science, Berkeley, CA, pp. 87-96 (1986).

[16] Kokkala, M., D. Baroudi, and W. Parker, "Upward Flame Spread on Wooden Surface Products: Experiments and Numerical Modeling," in *Fire Safety Science-Proceedings of the Fifth International Symposium*, International Association for Fire Safety Science, Melbourne, Australia, pp. 300-320 (1997).

[17] Lattimer, B., S. Hunt, H. Sorathia, M. Blum, T. Gracik, M. McFarland, A. Lee, and G. Long, "Development of a Model for Predicting Fire Growth in a Combustible Corner," *NSWCCD-TR-64-99/07*, U.S. Navy, West Bethesda, MD (1999).

[18] Foley, M. and D. Drysdale, "Heat Transfer from Flames between Vertical Parallel Walls," *Fire Safety Journal*, 24, pp. 53-73 (1995).

[19] Ahmad, T. and G. Faeth, "Turbulent Wall Fies," in *17th Symposium (International) on Combustion*, Combustion Institute, Pittsburgh, PA, pp. 1149-1160 (1979).

[20] Orloff, L., J. de Ris, and G. Markstein, "Upward Turbulent Spread and Burning of Fuel Surfaces," *Fifteenth Symposium (International) on Combustion*, The Combustion Institute, Pittsburgh, PA, 183 (1975).

[21] Hasemi, Y., "Experimental Wall Flame Heat Transfer Correlations for the Analysis of Upward Wall Flame Spread," *Fire Science and Technology*, 4, 2, pp. 75-90 (1984).

[22] Hasemi, Y., "Thermal Modeling of Upward Wall Flame Spread," *Fire Safety Science-Proceedings from the Fifth International Symposium*, Hempisphere Publishing, Gaithersburg, MD, pp. 87-96 (1986).

[23] Hasemi, Y., "Deterministic Properties of Turbulent Flmaes and Implications on Fire Growth," *INTERFLAM '88*, John Wiley and Sons, Cambridge, UK, pp. 45-52 (1988).

[24] Mitler, H., "Predicting the Spread Rates on Vertical Surfaces," *23rd Symposium (International) on Combustion*, The Combustion Institute, Pittsburgh, PA, pp. 1715-1721 (1990).

[25] Williams, F., C. Beyler, S. Hunt, and N. Iqbal, "Upward Flame Spread on Vertical Surfaces," NRL/MR/6180-97-7908, Navy Technology Center for Safety and Survivability, Chemistry Division (1997).

[26] Tewarson, A., "Generation of Heat and Chemical Compounds in Fires," *3rd Edition of the SFPE Handbook of Fire Protection Engineering*, Section 3, Chapter 4, National Fire Protection Association, Quincy, MA, USA (2002).

[27] ASTM E2058: *Standard Test Methods for Measurement of Synthetic Polymer Material Flammability Using a Fire Propagation Apparatus (FPA)* (2006), West Conshohocken, PA, USA: American Society for Testing and Materials.

[28] Quintiere, J, M. Harkleroad, and Y. Hasemi, "Wall Flames and Implications for Upward Flame Spread", *Combustion Science and Technology*, 48, pp. 191-222 (1986).

[29] Delichatsios, M., "Flame Heights in Turbulent Wall Fires with Significant Flame Radiation," *Combustion Science and Technology*, 39, 194-215 (1984).

[30] Panagiotou, J., "A Methodology for Flammability Diagrams," M.S. Thesis, University of Maryland.

[31] Spearpoint, M. and J. Quintiere, "Predicting the Piloted Ignition of Wood in the the Cone Calorimeter Using an Integral Model - Effect of Species, Grain Orientation, and Heat Flux," *Fire Safety Journal*, 36, 2001.

[32] Lyon, R. and J. Quintiere, "Criteria for piloted ignition of combustible solids", *Combustion and Flame*, Vol. 151, No. 4, Dec 2007.

[33] Wang, Y., J. Zhang, J. Jow, and K. Su, Analysis and Modeling of Ignitability of Polymers in the UL-94 Vertical Burning Test Condition, University of Science and Technology, Qingdao, China.

[34] Quintiere, J., "A Theoretical Basis for Flammability Properties", *Fire and Materials*, Vol. 30, 3, pp. 175-214 (2006).

[35] Roberts, A. and B. Quince, "A Limiting Condition for the Burning of Flammable Liquids," *Combustion and Flame*, 20, 245-251 (1973).

[36] Quintiere, J., "Surface Flame Spread," *3rd Edition of the SFPE Handbook of Fire Protection Engineering*, Section 12, Chapter 2, National Fire Protection Association, Quincy, MA, USA (2002).

[37] Quintiere, J., *Fundamentals of Fire Phenomena*, West Sussex, England: Wiley and Sons, Ltd. (2006).

[38] Incropera, F., D. DeWitt, T. Bergman, *Fundamentals of Heat and Mass Transfer*, Hoboken, NJ, USA: Wiley and Sons, Ltd. (2005).

[39] Kim, M. and J. Quintiere, "Predicting Polymer Burning using TGA/DSC", *5th Int. Seminar on Fire and Explosion Hazards*, Edinburgh, 23-27 April 2007.

[40] Stoliarov, S. and R. Walters, Determination of the Heats of Gasification of Polymers Using Differential Scanning Calorimetry, *Polymer Degradation and Stability*, 93, pp. 422-427 (2008).

[41] Ohlemiller, T. and J. Shields , "Aspects of the Fire Behavior of Thermoplastic Materials", *NISTIR 1493*, January 2008.

[42] Roper, F., C. Smith, and A. Cunningham, "The Prediction of Laminar Jet Diffusion Flame Sizes: Part II. Experimental Verification," *Combustion and Flame*, 29, pp. 227-234 (1977).